TRANSPARENT GLASS CERAMICS DOPED BY CHROMIUM(III) AND CHROMIUM(III) AND NEODYMIUM(III) AS NEW MATERIALS FOR LASERS AND LUMINESCENT SOLAR CONCENTRATORS

Research supported by U.S. Army
under Contract No. DAJA 45-85-C-0051

2nd & 3rd Interim

Annual Report
~~1.10.87 - 30.9~~.86

Submitted by

Professor Renata Reisfeld
Department of Inorganic and Analytical Chemistry
The Hebrew University of Jerusalem
Jerusalem 91904 Israel

to

European Office of the U.S. Army
223/231 Old Marylebone Rd.
London WC1 5TH
England

and

Army Materials and Mechanic
Research Center, Watertown,
Massachusetts 02172
U.S.A.

This work was performed together with Alla Buch, Mehdi Bouderbala, Georges Boulon, Esther Greenberg, Moshe Ish-Shalom, Anna Kisilev, and Anne-Marie Lejus.

CONTENTS

Page	
4	Abstract
5	Preparation, characterization and properties of transparent glass ceramics.
19	Time-resolved and temperature-dependent spectra of chromium(III) in glasses and spinel-type glass-ceramics.
26	Transparent glass-ceramics doped by chromium(III): Spectroscopic properties and characterization of crystalline phases.
52	Spectroscopy and EPR of chromium(IXI) in mullite transparent glass-ceramics.

ABSTRACT

Transparent glass ceramics were prepared in the system Li_2O-Al_2O_3-SiO_2, MgO-Al_2O_3-SiO_2 and ZnO-Al_2O_3-SiO_2 using TiO_2, ZrO_2 and P_2O_5 as nucleators. The major crystalline phases in these samples were spinel, gahnite, β-quartz solid solutions and petalite-like-phase. These were doped with Cr(III) and spectroscopic properties measured. The efficiency of luminescence in these glass ceramics was very high compared to glass samples, viz. ca. 50% in β-quartz, 75% in petalite-like-phase and close to unity in gahnite. For practical purposes the results may be important in designing luminescent solar concentrators and lasers based on Cr(III).

Time-resolved spectroscopy of Cr^{3+}-doped glasses or spinel-type glass ceramics with titanium and titanium-zirconium as nucleating agent allows us to distinguish between the long-lived ^2E and short-lived $^4T_2$ states. Temperature dependence and time resolution permit us to locate the various levels and presence of aggregates of Cr^{3+} in these systems.

Several types of transparent glass-ceramics doped by Cr(III) were prepared in SiO_2-Al_2O_3-RO (R = Mg, Ca, Zn) systems. The crystalline phases obtained after appropriate heat treatments were determined by X-ray diffraction. The spectroscopic behavior of Cr(III) allows characterization of the crystalline phases in which Cr(III) is incorporated by analogy with crystals.

Mullite glass-ceramics were prepared with varying concentrations of Cr(III). The X-ray absorption, emission and EPR spectra reveal that the most defined crystals are formed at the lowest concentration of Cr(III). The concentration quenching of the luminescence is small and the quantum efficiencies high as compared with glasses.

PREPARATION, CHARACTERIZATION AND PROPERTIES OF TRANSPARENT GLASS CERAMICS

Transparent glass ceramics were prepared in the system Li_2O-Al_2O_3-SiO_2, MgO-Al_2O_3-SiO_2 and ZnO-Al_2O_3-SiO_2 using TiO_2, ZrO_2 and P_2O_5 as nucleators. The major crystalline phases in these samples were spinel, gahnite, β-quartz solid solutions and petalite-like-phase. These were doped with Cr(III) and spectroscopic properties measured. The efficiency of luminescence in these glass ceramics was very high compared to glass samples, viz. ca. 50% in β-quartz, 75% in petalite-like-phase and close to unity in gahnite. For practical purposes the results may be important in designing luminescent solar concentrators and lasers based on Cr(III).

1. INTRODUCTION

Glasses containing Cr(III) as potential materials for solar concentrators were studied intensively [1]. The strong absorption of Cr(III) extending over almost the entire visible spectrum makes it a priori a good candidate for the capture of solar energy. However, the glassy phase seems to provide a medium with too low quantum efficiencies of fluorescence (less than 25% [2-4]), while there are indications of very high quantum efficiencies in crystalline phases.

Glass ceramics in which Cr(III) is concentrated in crystallites dispersed in a glassy phase and having dimensions smaller than the wavelength of visible radiation, should provide transparent materials of high quantum efficiencies, from which plates can be made quite readily. This was indeed demonstrated qualitatively in transparent glass ceramics containing mullite [2] melted at temperatures above 1650°C. The main objective of the present study was to prepare transparent glass ceramics containing Cr(III) in different crystalline phases (temperature of melting preferably below 1600°C), to determine the absorption and emission characteristics of Cr(III) in these materials and to compare them with the characteristics of Cr(III) in glasses.

Glasses in the basic Li_2O-Al_2O_3-SiO_2, MgO-Al_2O_3-SiO_2 and ZnO-Al_2O_3-SiO_2 systems were prepared. TiO_2 was first used as a nucleator, but when it turned out that it was causing colouration, it was attempted to reduce its quantities. TiO_2, ZrO_2 and P_2O_5 were then employed as nucleators, alone or in combination with each other. The crystalline phases produced in the transparent glass ceramics were: spinel, gahnite, β-quartz solid solutions and petalite-like phase. Comparison of the properties of gahnite and spinel is of interest since they have the same spinel type structure, which in gahnite Zn ions replace all Mg ions.

During preparation of the samples for measurements of the spectroscopic properties it was noticed that some of the samples were very hard. Quantitative measurements confirmed these observations. Microhardness measurements were carried out on several modifications in composition of the glasses and glass ceramics. However, these results will not be detailed in the present paper since certain aspects still need further elaboration.

2. EXPERIMENTAL

The compositions of the glasses intended for the preparation of transparent glass ceramics lie on the $RO(R_2O):Al_2O_3$=1:1 or on its Al_2O_3 side of the high silica end of the diagram.

The selected compositions are shown in Table 1.

The glasses of the desired compositions were prepared by thoroughly dry mixing of the batch ingredients by hand, in a porcelain mortar, for 15-20 minutes, in batches to yield about 100 grams of glass. The raw materials were high purity oxides exept for $LiOH.H_2O$ and $NH_4H_2PO_4$ as sources of Li_2O and P_2O_5, respectively. As sources of SiO_2 and Al_2O_3 - Belgian glass sand, "Sibelco" (99.8% SiO_2) and of Alcoa A-16SG (>99.5% Al_2O_3) respectively, were used.

Melting of the glasses was done in alumina crucibles at temperatures of 1560-1580°C, in an electric furnace, for 2-3 hours. The melted glass was cast into steel moulds and pressed into plates approximately 5mm thick. These were immediately placed in a furnace at 650°C for annealing; the furnace was turned off and sample cooled down with it.

Conditions of further heat treatment were determined using mass crystallization in an electric furnace. Heat treatment was done in two stages. The initial stage varied between 700-800°C (4-10 hrs). The temperature of the second stage (crystallization) was selected to be the highest possible above which the glass ceramic lost transparency. Heating rate was 3-5°C/min. "Nucleation" and crystallization temperatures, t_1 and t_2 respectively, and soaking times are shown in Table 1.

The crystalline phases present after heat treatment were determined by X-ray diffraction of powdered samples using a Philips diffractometer with CuKα radiation with Ni filter.

The details of the instrumentation and spectroscopic measurements - absorption, excitation and emission spectra - are given in references [3,4].

Linear thermal expansion coefficients were determined using a Chevenard Model 50 dilatometer.

3. RESULTS AND DISCUSSION

3.1 Phase Compositions

The main crystalline phases present in the glass ceramic samples are shown in Table 1.

Glasses 3 and 7

The original compositions of glasses 3 and 7 represent the highest and lowest silica contents, respectively, in the cordierite field in the $MgO-Al_2O_3-SiO_2$ phase diagram. Three crystalline phases were found in both compositions after the appropriate heat treatments: β-quartz ss (q), spinel (s) and magnesium-aluminotitanate (Mat). (Fig. 1).

The similarity in the phases found in the two compositions suggests the likelihood of a phase separation process (liquation) of the original glass during heat treatments. In the process a high-silica glassy phase crystallized to form β-quartz ss, while the high-cation glassy phase yielded spinel and Mat.

The relative quantities of spinel and Mat are approximately the same in base glasses 3 and 7, but the quantity of the β-quartz ss phase is higher in glass no. 7. It may be assumed that the high cation glassy phase has about the same composition in both samples; but the high silica phase in sample no. 7 is enriched with MgO and Al_2O_3, still maintaining the β-quartz structure; while the same glassy phase in sample no. 3 is enriched with silica, making it less amenable to crystallization. The transparent glass ceramic no. 3 is thus expected to consist of a higher proportion of glassy phase.

The linear thermal expansion coefficients of the two glass ceramic samples are 37 and 47 x 10^{-7} (1/°C) for glass ceramics no. 3 and 7, respectively.

The substitution of part of the TiO_2 by ZrO_2 (in glasses 7Z and 3-1) resulted in a change in the liquation process and in the composition of the coexisting glassy phases. In the transparent glass ceramics petalite-like phase (plp), β-quartz ss and ZrO_2 were found. It is known [5] that plp appears during the initial stages of crystallization of TiO_2 -containing liquated glasses and of glasses in the high magnesium low silica part of the $MgO-Al_2O_3-SiO_2$ system located near the liquation field. It probably represents a series of solid solutions on the basis of $MgO \cdot SiO_2$ obtained as a result of substitution $2Si^{4+} \rightarrow 2Al^{3+} + Mg^{2+}$ into a layered structure, or introduction of $(AlO_4)Mg_{0.5}$ between layers [6].

Introduction of ZrO_2 into the composition of the glass promotes the redistribution of the components during liquation: the structure of the high silica phase is similar to the one of β-quartz (as in glasses no.3 and 7); the structure of the high cation phase is similar to that of pip. Thus, in composition no. 3-1 β-quartz ss is the base crystalline phase, and in composition no. 7Z pip is the base. In both compositions ZrO_2 appears in the crystalline form (fig. 1).

The substitution of part of the TiO_2 by ZrO_2 and P_2O_5 (glass no. 7P) resulted in the transparent glass ceramic containing only $AlPO_4$. One may suppose that the mechanism of crystallization changes: the liquation of the glass does not take place: P^{5+} forms with Al^{3+} stable groups which crysatllize after suitable heat treatment.

Glasses 4 and 5

The composition of glass no. 4 was selected in the system $ZnO-Al_2O_3-SiO_2$ with the purpose of obtaining gahnite-containing transparent glass ceramic. Part of ZnO was substituted by Li_2O in order to decrease the melting temperature. However, β-quartz ss was found in it as the major crystalline phase. Increasing the amount ZnO and TiO_2 (composition no. 4-1) the phase composition of the transparent glass ceramic changed and gahnite was found to form the major crystalline phase with some β-quartz ss as minor phase (fig. 1). This fact suggests that a liquation mechanism operates as in no. 3: the high silica glassy phase gives β-quartz ss, while the high cation phase - yields gahnite, having the same crystallographic structure as spinel. When the Li_2O content was increased in the original glass - β-quartz ss containing transparent glass ceramic was formed (composition no. 5). TiO_2 and ZrO_2 stayed in the residual glassy phase at these temperatures. The P_2O_5 content in composition no. 5 is worth noting. The isostructural nature of the

crystalline phases in the $(SiSi)O_4$ and $(AlP)O_4$ makes it practically impossible to distinguish between the analogous structures in the two chemical systems by powder XRD. It may thus be that part of the β-quartz ss may actually consist of an $(AlP)O_4$ analog of this structure. This glass ceramic (without Cr(III)) is colourless owing to the low TiO_2 content and has a practically zero thermal expansion coefficient.

3.2 Spectroscopic Measurements

Detailed absorption, excitation and emission measurements were performed on samples no. 3, 4-1, 5 and 7Z, in which the major crystalline phases were spinel, gahnite, β-quartz ss and petalite-like-phase (plp), respectively. Full details of the results and discussion were given elsewhere [3,4]. Only the main results and conclusions will be given here.

The absorption of the glasses before crystallization consists of two broad bands peaking at 450 nm due to the $^4A_2 \longrightarrow {}^4T_1$ transition and at 650 nm due to the $^4A_2 \longrightarrow {}^4T_2$ transition. The absorption spectrum is very similar to that described in detail in ref. [6]. The absorption spectra of the species having high concentrations of TiO_2 contain additional absorption in the region of 300-500 nm, probably due to the presence of Ti^{3+}, which might be formed during the crystallization process. The glass ceramics samples in which ZrO_2 is the main nucleating agent are almost free from this absorption.

Typical excitation spectra of a glass ceramic - consisting of spinel - is shown in fig. 2. The excitation curves depend on the emission wavelength used to measure it. The curves obtained at emission wavelengths of 770 and 830 nm are typical to the Cr(III) in the glassy phase and those measured at 688 and 705 nm are characteristic to the Cr(III) in the crystalline phase.

The emission spectra of the four glass-ceramic samples are shown in fig. 3. Similar to the excitation spectra the emission spectra are dependant on the excitation wavelengths.

The emission spectra of the spinel containing glass ceramic (no. 3) is presented in fig. 3a. For excitations at 475 and 627 nm they are composed of a structured part at around 680 nm due to transition from ^2E and a broad emission in the range 650-950 nm from $^4T_2$.

The emission spectrum of the gahnite containing sample (4-1) is given in fig. 3b. Excitation at 475 nm results in a very weak fluorescence consisting of four sharp bands between 670 and 740 nm and a broad emission up to 950 nm. A similar picture is obtained when the sample is excited at 545 nm, however, the fluorescence is more intense by a factor of 10 and the main emission comprises 4 sharp peaks at 675, 689, 697 and 708 nm with a very weak broad-band emission at longer wavelengths. When excited at 625 nm, only one sharp peak is obtained at 705 nm and a broad emission extending up to 950 nm.

The emission spectra of β-quartz ss containing sample (5) is given in fig. 3c. Excitations of 625 and 595 nm give rise to a broad emission peaking around 830 nm due to $^4T_2 \rightarrow {}^4A_2$ and a slight contribution of the emission arising from ^2E with two peaks between 625 and 706 nm. This contribution from ^2E, single sites and pairs, is much less than in the gahnite and spinel samples.

The emission spectrum of petalite-like glass ceramic (72) is shown in fig. 3d. Excitation at 475 nm and 625 nm results in a broad emission up to 950 nm from $^4T_2 \rightarrow {}^4A_2$ and weak emission from ^2E around 698 and 717 nm. The emission spectrum for excitation at 570 nm is mainly composed of the ^2E emission peaking at 690 and 720 nm.

The efficiency of the total luminescence in gahnite was found to be ~1 at room temperature. The quantum efficiency of Cr(III) in the glassy material of the same composition from which the glass ceramic was obtained was lower by a factor of 10. This dramatic increase of the quantum efficiency in the crystalline phase is a result of the decrease of the non- radiative de-excitation in the ordered system.

The quantum efficiencies found for Cr(III) in β-quartz was 50% and in the petalite-like phase 75%.

Calculations were also made of the ligand field parameters for Cr(III) in glass ceramics, glasses, crystals and complexes [3]. From these the following conclusions were drawn about the relative strength of the ligand fields: the highest ligand field is observed in gahnite, which is comparable to ruby. Spinel and petalite like phase are subjected to ligand fields similar to alexandrite crystal and Cr-oxalate complex. In β-quartz Cr(III) is subject to a field similar to that for yttrium gallium garnet.

From the practical point of view, the findings presented here may be important in designing luminescent solar concentators and lasers based on Cr(III).

Table 1 The compositions of investigated glasses (mol %), heat treatment and crystalline phases in transparent glass ceramics.

	SiO_2	Al_2O_3	MgO	Li_2O	ZnO	TiO_2	ZrO_2	P_2O_5	Temp. of nucleation t_1 crystallization t_2 and soaking time	Crystalline phases in glass-ceramics: major	minor
3	58.7	16.7	17.8	-	-	6.7	-	-	750-10h 980- 2h	spinel	β-quartz ss mat**
3-1	58.7	16.7	17.8	-	-	3.7	3.0	-	750-10h 900- 2h	β-quartz ss	plp**
4	75.8	11.9	7.2	3.0	1.0	1.0	1.5	-	750-10h 870- 2h	β-quartz ss	ZrO_2
4-1	72.8	11.9	-	7.2	4.7	1.9	1.5	-	750-10h 870- 2h	gahnite	β-quartz ss ZrO_2
5	65.8	17.1	1.9	7.9	1.2	1.7	1.1	3.2	800- 4h 880- 2h	β-quartz ss	-
7	49.1	19.9	20.1	-	-	10.9	-	-	750-10h 920- 2h	β-quartz ss spinel	mat*
7Z	49.1	19.7	21.9	-	-	6.0	3.2	-	750-10h 900- 2h	plp**	β-quartz ss ZrO_2
7P	49.4	19.8	20.7	-	1.4	2.6	2.8	3.3	750-10h 900-2h	$AlPO_4$	-

* mat - magnesium alumotitanate ss
** plp - petalite-like phase

REFERENCES

1. Reisfeld R., and Jørgensen C.K., Struc. Bonding 49 (1982), 1.

2. Beall Y.H., MacDowell J.F. and Taylor M.P., "Transparent glass-ceramics containing mullite", U.S. Patent 4,396,720 (2 Aug. 1983).

3. Reisfeld R., Kisilev A., Greenberg E., Buch A., Ish-Shalom M., "Spectroscopy of Cr(III) in transparent glass-ceramics containing spinel and gahnite", Chemical Physics letters, vol. 104, no.(2,3)p. 153-156, 1984.

4. Kisilev A., Reisfeld R., Greenberg E., Buch A., Ish-Shalom M., "Spectroscopy of Cr(III) in β-quartz and petalite-like transparent glass-ceramics: ligand field strength of Cr(III)", Chemical Physics letters, vol. 4, 405-408, 1984.

5. Varshal B.Y., Baiburt L.Y., Gelberger A.M., Malakhovskaja N.N., Naumkin A.P., "Synthesis of metastable Mg- and Zn- containing petalite -like phases", Isv. Akad. Nauk SSSR, 1971 7(4), 712 deposit VINITI N2482-71.

6. Reisfeld R., J. Less-Common Mat., 93(1083), 243.

7. Pavlushkin N.M., Ellern Y.A., "Investigation of crystallize process ZrO_2-containing glasses", Isvestija AN SSSR, Neorgan. mat. 11(10) 1975, 1869-1872.

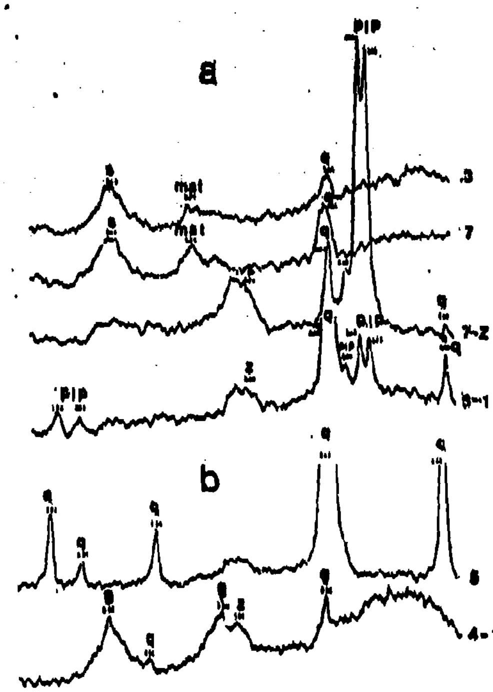

Fig. 1 X-Ray diffraction of the transparent glass-ceramics

s - spinel, g - gahnite, plp - petalite-like phase
q - β-quartz solid solutions, mat - magnesium-alumotitanates, z - zirconia

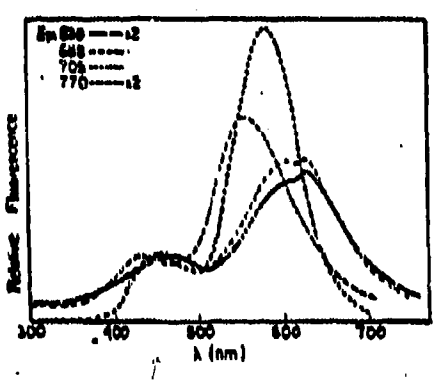

Fig. 2 Excitation spectra of spinel for various emission at room temperature.

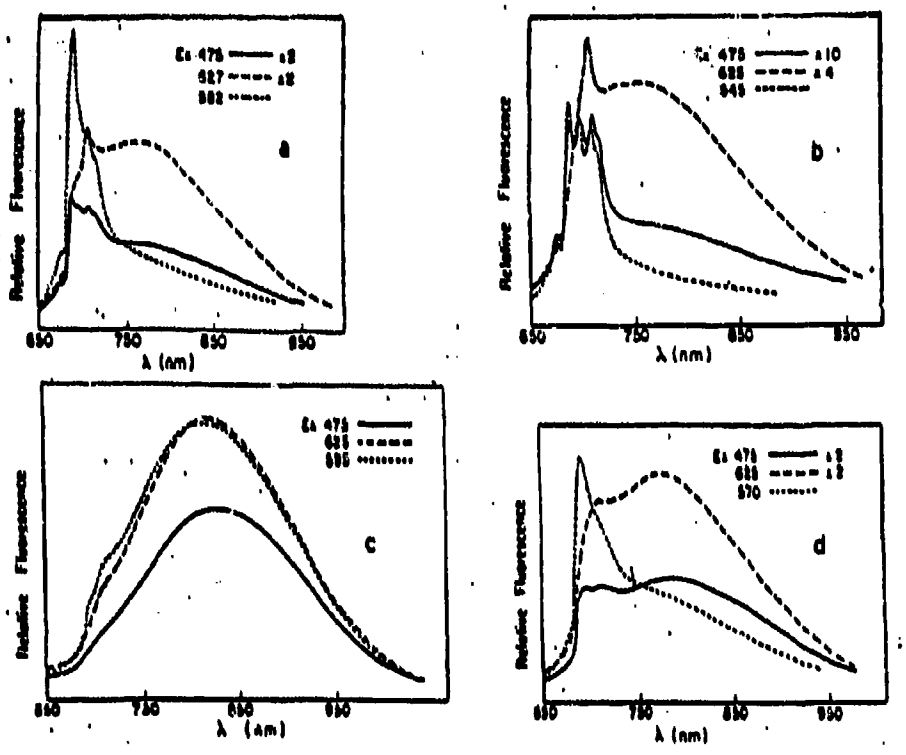

Fig. 3 Emission spectra of transparent glass-ceramics for various excitations at room temperature:
a) spinel-containing glass-ceramic (no. 3)
b) gahnite-containing glass-ceramic (no. 4-1)
c) β-quartz ss-containing glass-ceramic (no. 5)
d) petalite-like phase-containing glass-ceramic (no. 7Z)

TIME-RESOLVED AND TEMPERATURE-DEPENDENT SPECTRA OF CHROMIUM(III) IN GLASSES AND SPINEL-TYPE GLASS-CERAMICS

Time-resolved spectroscopy of Cr^{3+}-doped glasses or spinel-type glass ceramics with titanium and titanium-zirconium as nucleating agent allows us to distinguish between the long-lived ^2E and short-lived $^4T_2$ states. Temperature dependence and time resolution permit us to locate the various levels and presence of aggregates of Cr^{3+} in these systems.

INTRODUCTION

We have recently shown that Cr^{3+}-doped glasses of special composition can be converted by appropriate thermal treatment (say around 1570°C) to transparent glass-ceramics containing crystallites much smaller than the wavelength of visible light [1-5]. The potential uses of these materials in tunable lasers and in luminescent solar concentrators have also been discussed [6]. In order to establish the relative positions of the $^4T_2$ and ^2E levels and their shifts when the glassy material is converted to the mainly crystalline glass-ceramic two materials A and B of the following composition in molar percent were studied:

A. 58.7 SiO_2; 16.7 Al_2O_3; 17.8 MgO; 6.7 TiO_2; 0.03 Cr_2O_3

B. 49.1 SiO_2; 19.7 Al_2O_3; 21.9 MgO; 5.0 TiO_2; 3.2 ZrO_2; 0.03 Cr_2O_3.

In what follows the original glass samples are called Ag and Bg and the glass-ceramics obtained after thermal treatment Ac and Bc.

The preparation of these materials of the spinel type has been described [1]. For comparison we have also grown crystals with the formula:

Spinel $MgAl_2O_4(Cr^{3+})$, $Mg_2TiO_4(Cr^{3+})$, $Mg_2(Ti_xZr_{1-x})O_4(Cr^{3+})$, $Mg_{1.2}Ti_{0.2}Al_{1.6}O_4(Cr^{3+})$.

For the spectroscopic measurement we have used a quantal YAG-Nd pulsed laser followed by a tunable dye laser to scan the required wavelength. The detailed experimental data were similar to those described in ref. [7]. The temperature of the measurement ranged from 4.4 K to room temperature.

RESULTS

Fig. 1 presents a comparison of the emission spectra of Ag and Ac samples for titanium only under several excitation wavelengths at 4.4 K. The glassy sample Ag is characterized by two main emission bands, one peaking at 711 nm due to the $^2E \rightarrow {}^4A_2$ transition and a broad-band emission at around 800 nm due to the $^4T_2 \rightarrow {}^4A_2$ transition. The positions of the two bands are independent of their excitation wavelength. None of the emission spectra presented here is corrected for the spectral response of the photomultiplier and the analysing grating: the corrected spectra of the $^4T_2 \rightarrow {}^4A_2$ emission are shifted to longer wavelength. For instance the maximum at 800 nm should be shifted to 927 nm at room temperature and to 984 nm at 77 K under 514.5 nm Ar excitation by using a germanium photodiode. In the glass-ceramics under similar excitation the broad-band emission disappears and only the ^2E emission is present. This emission is split into several components due to single and associated ions as discussed below.

We also show in fig. 1 a comparison of the emission spectra between the glass and glass-ceramics Bg and Bc containing zirconium in addition to titanium. The main features of these spectra resemble Ag and Ac. The room-temperature emission spectrum of the glass lacks the sharp ^2E emission due to the fact that the high vibrations of states of ^2E is more completed population of $^4T_2$ which is the major emitting state at room temperature.

Fig. 2 presents the time-resolved emission spectra of the glassy and crystalline titanium samples Ag and Ac. Similar measurements for the zirconium exhibit identical behavior. As mentioned above, the short-lived $^4T_2 \rightarrow {}^4A_2$ transition present in the glassy phase is absent in the glass-ceramics at 4.4 K. In addition the glass-ceramics reveal a gradual time-dependent disappearance of the band peaking at 706 nm and an increase of the bands at 686.5, 689.7 and 693.5 nm. From this behavior we conclude that the 706 nm band is due to short-lived pairs or higher aggregates which are antiferromagnetically coupled [1-3] while the long-lived band around 690 nm is due to $^2E \rightarrow {}^4A_2$ emission from single Cr^{3+} ions. It should be mentioned that in the glassy phase the most pronounced band is due to aggregates.

The decay time of all samples were measured at 4.4 K and at room temperature. A non-exponential behavior of the decay curves is observed

in all cases, mainly because of the multiplicity of Cr^{3+} sites. In the glassy sample the shortest branch of the decay curve of the $^4T_2 \rightarrow {}^4A_2$ transition (800 nm) can be fitted to τ = 14 µs at 4.4 K and the longer branch due to $^4T_2 \rightarrow {}^4A_2$ has τ = 47 µs under 600 nm excitation and τ = 140 µs under 570 nm excitation due to the thermalization of ^2E and $^4T_2$ states.

The decay curves at 705 nm due to the $^2E \rightarrow {}^4A_2$ transition exhibit a long-time component of about 3 ms.

The lifetime behavior of the Ac and Bc samples are presented in fig. 3. At 4.4K, 705 nm emission due to aggregates under 570 and 600 nm exhibits a long component of 3.4 ms. The 691 nm emission under excitation into 688 nm ^2E has a lifetime of 8.4 ms due to single ions. At room temperature for the Ac a strong contribution of $^4T_2$ is observed, as reflected by shorter lifetime which consists of two components 50 and 430 µs.

The zirconium containing glass ceramics shows a longer decay than the corresponding titanium doped sample. The longest lifetime is 16.6 ms on excitation to 570 nm and emission at 688 nm. This long time arises from Cr^{3+} single ions positions at high symmetry sites in the titanium-zirconium samples.

It should be noted that Cr^{3+} ions in lower symmetry sites have lifetimes as short as 6 ms.

A qualitative summary of these results is given in fig. 4 which represents Cr^{3+} sites for single ions. The ^2E state is above $^4A_2$ and is unchanged for Cr^{3+} in different environments. $^4T_2$ may change its position considerably in various environments and it lies above ^2E in the crystalline phase and at the same position or slightly lower in the glassy phase. The pairs and more highly associated ions are not represented in the figure; as noted above they have shorter lifetimes than do Cr^{3+} ions in single positions. A similar result has been found for ruby [8].

A comparative study of Cr^{3+} behavior in glass-ceramics and in "real" crystals of similar composition is now in progress.

This work was performed in collaboration with the group of Professor Georges Boulon at the University of Lyon.

REFERENCES

1. R. Reisfeld, A. Kisilev, E. Greenberg, A. Buch and M. Ish-Shalom, Chem. Phys. Letters 104 (1984) 153.
2. A. Kisilev, R. Reisfeld, E. Greenberg, A. Buch and M. Ish-Shalom, Chem. Phys. Letters 105 (1984) 405.
3. F. Durville, B. Champagnon, E. Duval, G. Boulon, F. Gaume, A.F. Wright and A.N. Fitch, Phys. Chem. Glasses 25 (1984) 126.
4. F. Durville, B. Champagnon, E. Duval and G. Boulon, J. Phys. Chem. Solids 46 (1985) 701.
5. B. Champagnon, F. Durville, E. Duval and G. Boulon, J. Luminescence 31/32 (1984) 345.
6. R. Reisfeld, Materials Science and Engineering 71 (1985) 375.
7. F. Durville, G. Boulon, R. Reisfeld, M. Mack and C.K. Jørgensen, Chem. Phys. Letters 102 (1983) 393.
8. F. Imbusch, Energy Transfer Processes in Condensed Matter, ed. B. Di Bartolo, NATO ASI Ser.B, Physics, Vol.114 (Plenum Press, New York, 1984) p.471.

Figure Captions

Fig. 1 Emission spectra of Ag (a) and Ac (b), and emission spectra of Bg (c) and Bc (d) under various laser excitations at 4.4 K and also at room temperature for the Bg sample.

Fig. 2 Time-resolved spectra of Ag (a) and Ac (b) under 570 nm laser excitation at 4.4 K.
D = delay time.
The gate width was 100 μs.

Fig. 3 Decay curves of Ac (b) and Bc (a) for various emission wavelengths under several laser excitations.

Fig. 4 Schematic configurational coordinate curves for Cr^{3+} single ions in crystallites (a) and in glasses (b).

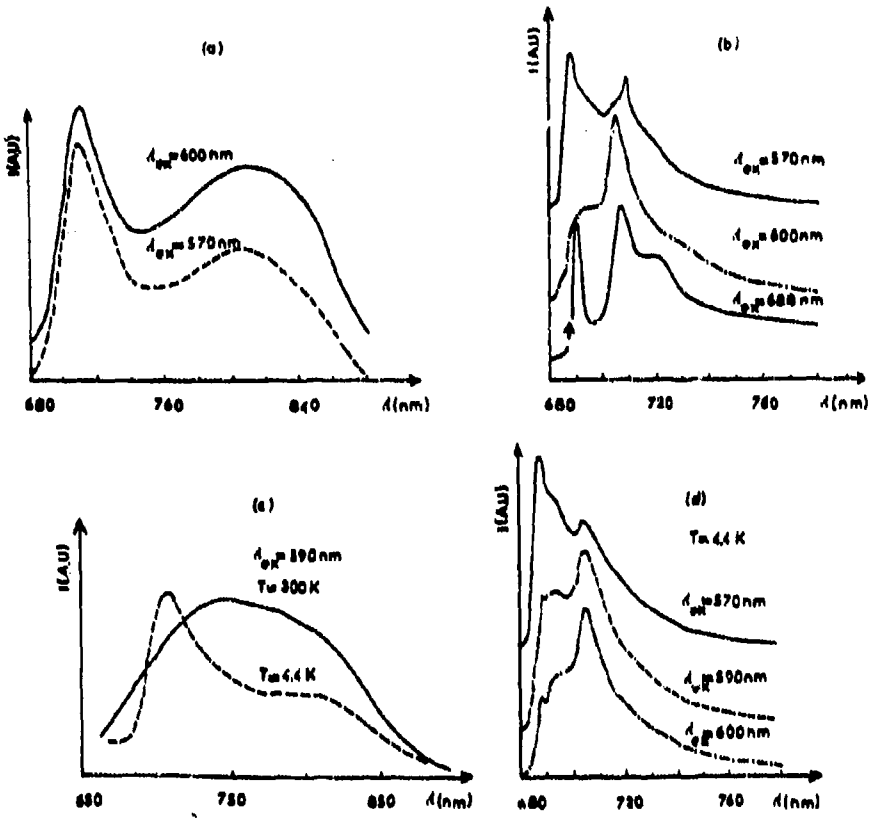

Fig. 1

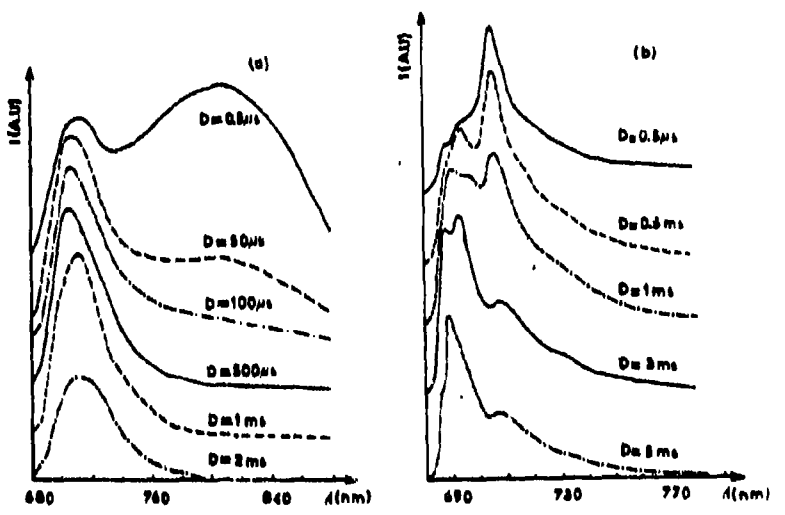

Fig. 2

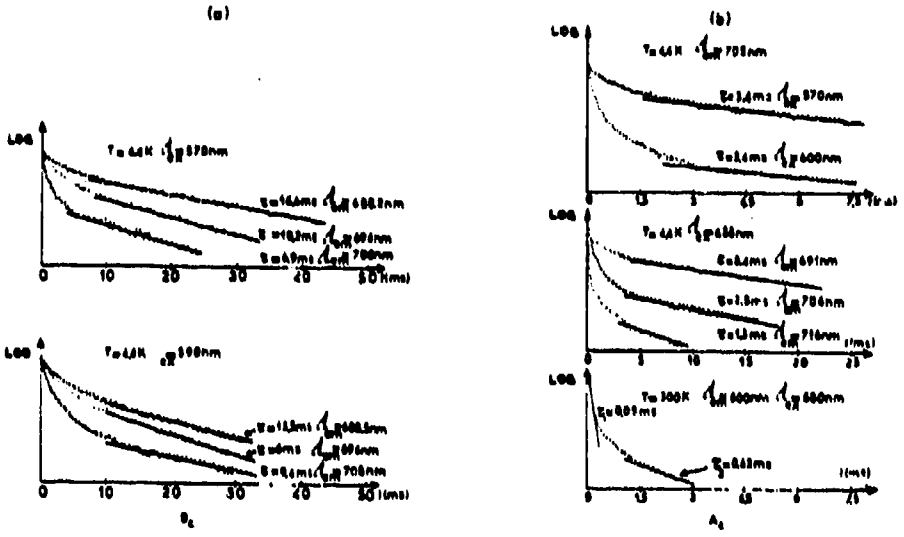

Fig. 3

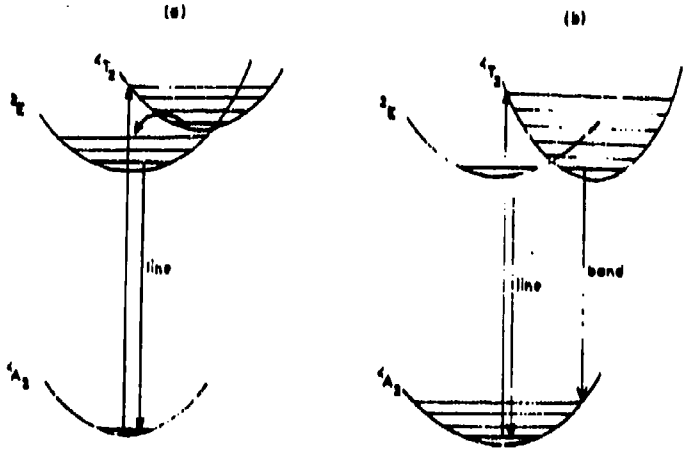

Fig. 4

Accepted for publication in the Journal of Non-Crystalline Solids
To be published in 1987

TRANSPARENT GLASS-CERAMICS DOPED BY CHROMIUM(III); SPECTROSCOPIC PROPERTIES AND CHARACTERIZATION OF CRYSTALLINE PHASES*

R. Reisfeld** and A. Kisilev

Department of Inorganic and Analytical Chemistry
The Hebrew University of Jerusalem, Jerusalem 91904, Israel

and

A. Buch and M. Ish-Shalom

Israel Ceramic and Silicate Institute
Technion City, Haifa 32000, Israel

Abstract

Several types of transparent glass-ceramics doped by Cr(III) were prepared in SiO_2-Al_2O_3-RO (R = Mg, Ca, Zn) systems. The crystalline phases obtained after appropriate heat treatments were determined by X-ray diffraction. The spectroscopic behavior of Cr(III) allows characterization of the crystalline phases in which Cr(III) is incorporated by analogy with crystals.

* Supported by US Army Contract DAJA 45-85-C-0051
** Enrique Berman Professor of Solar Energy

Introduction

The importance of transparent glass-ceramics doped by Cr(III) as potential new materials for LSC (luminescent solar concentrators) and tunable lasers has been recently reviewed [1,2]. In a number of papers [3-8] using absorption and steady state luminescence, it has been shown that Cr(III) exhibits exceptionally high quantum efficiency of luminescence as compared to that in glasses of the same compositions.

In octahedral symmetry, d^3 systems like chromium(III) have three excited quartet (total spin quantum number S=3/2) states above the groundstate $^4A_2$ and a large number of excited doublets (S=1/2). The first excited state is either $^4T_2$ in "low-field" situations, where the sub-shell energy difference Δ between the two strongly anti-bonding d orbitals (e) and the three roughly non-bonding orbitals (t_2) is lower than the energy difference between ^2E and $^4A_2$ determined by effects of interelectronic repulsion; or it is ^2E in the "high-field" situation, where Δ is larger than the latter expression for spin-pairing energy. This distinction is relatively clear-cut in absorption spectra, but is modified by the Franck-Condon principle in luminescence, where the sub-shell configuration $(t_2)^2(e)^1$ of $^4T_2$ containing one anti-bonding electron has an energy above the groundstate $^4A_2$ dependent on the 18 internuclear distances between the chromium nucleus and the 6 nearest-neighbour nuclei. In particular, the scaling of all internuclear distances by the same factor slightly above 1 corresponds to a lower value of Δ and a lower excitation energy above $^4A_2$. On the other hand, ^2E has to a high precision the same sub-shell configuration $(t_2)^3$ as the groundstate $^4A_2$ and provides roughly parallel potential surfaces and a minor Stokes shift of the luminescence [1]. Hence, simultaneous emission may occur from ^2E and from $^4T_2$ at an energy considerably lower than the maximum of the broad absorption band. Also the time-evolution (decay curve) of the luminescence may deviate strongly from exponential behaviour, because energy is stocked in the ^2E state having life-times typically in the 10^{-3}s range, whereas the oscillator strength f (usually a few times 10^{-4}) of the spin-allowed transition from $^4T_2$ to $^4A_2$ corresponds to a radiative life-time in the 10^{-5}s range. The observed life-time of the $^4T_2$ luminescence (if detected at all) may be much shorter, due to non-radiative relaxation processes.

Comparison of the Δ values in Table 1 shows that the ligand field of Cr(III) in the crystalline phase of the glass-ceramics is higher than in the glassy phase or in glasses, and its value is comparable to that of Cr(III) in ruby and alexandrite. The ^2E level is some 1000 to 3000 cm^{-1}

below the minimum of the $^4T_2$ potential surface. Such a situation permits thermal equilibration between two levels, as has been found previously in many complexes and crystals, also such containing lanthanides and bismuth (III).

Later, it was shown [9] by time resolved spectroscopy of Cr(III) doped spinel and petalite-like phase types of glass-ceramics, that this method enables a more precise distinction of the ^2E and $^4T_2$ energy levels of Cr(III) and of the equlibrium between the populations of the two levels.

In the present work, a systematic study of the dynamic behaviour of Cr(III) luminescence was performed and an attempt to relate the spectroscopic properties of Cr(III) and the structure of the surrounding crystalline phases, was made.

I. Experimental procedure and results

I A. Preparation of glass-ceramics

The starting compositions of the glasses from which glass-ceramics were prepared, are given in Table 2.

TiO_2 and ZrO_2 were used as nucleators, separately or in combination. In the case of sample M, Cr_2O_3 itself plays the rôle of nucleator, not needing any additional TiO_2 or ZrO_2. The Cr_2O_3 concentrations, given in Table 2 in mole percent, correspond approximately to $1.1 \cdot 10^{19}$ Cr(III) ions/cm^3.

The raw materials were high purity oxides with the exception of $NH_4H_2PO_4$ used as source of P_2O_5. Belgian glass sand Sibelco (99.8 wt % SiO_2) and Alcoa A-16SG (greater than 99.5 wt % Al_2O_3) were used as SiO_2 and Al_2O_3.

The glasses were melted in Al_2O_3 crucibles at 1550 to 1560 °C in an electric furnace for 2 to 3 hours. The melts were cast into steel moulds and pressed into plates approximately 5 mm thick. These were immediately placed in a furnace at 500 °C for annealing; the furnace was turned off and the samples were cooled at the cooling rate of the furnace.

The addition of TiO_2 produces a greyish-yellowish shade of the usual green colour of Cr(III) doped glasses. We also prepared glasses of the same compositions, except for absence of Cr(III). The refractive indices of the glasses varied within the interval 1.63 to 1.65.

Conditions for further heat treatment were determined, using mass crystallization in an electric furnace. The heat treatment was carried out in two stages. The initial stage (nucleation) was carried out for 10 hours at 730 to 800 °C. The temperature just below which the glass-ceramics loses its transparency was selected for the second stage (crystallization). The heating rate for each stage was 3 to 5 °C/min. The nucleation temperatures t_1, the crystallization temperatures t_2 and the soaking times are shown in Table 2.

All the samples were transparent after heat treatment and the colour of most of them became more grayish. The TiO_2 - including samples darkened to a varying extent, depending on the TiO_2 concentration. It is caused either by the possible formation of Ti^{3+}; or by some other process [10] which is not well understood.

Identical heat treatments were performed on the undoped samples.

The refractive indices after heat treatment varied within 1.66-1.68.

IB X-ray diffraction measurements

The crystalline phases present after heat treatment were determined by x-ray diffraction of powdered samples using CuK_α tube with Ni-filter in a Phillips diffractometer. The x-ray diffraction spectra given in Fig. 1 were interpreted using the ASTM diffraction file.

The crystalline phases obtained are indicated in Tables 2 and 3. In each sample, in addition to crystalline phases, residual glass was also observed.

IC Spectroscopic measurements

Square samples of 10mm edge and 3mm thickness were cut from all the undoped and doped glasses and glass-ceramics. The surfaces as well as one narrow edge were polished for optical measurements.

The details of the spectroscopic measurements (absorption, excitation and emission spectra) have been given in [3,4].

Absorption spectra

Absorption spectra of samples were measured on a Cary-219 spectrophotometer. Samples of glass and glass-ceramics doped with Cr^{3+} were measured, using as blanks identical undoped samples of glass or glass-ceramics respectively

It should be noted that glass-ceramics containing titanium ions become darker, after heat treatment, than the corresponding glasses. The absorption at wavelength shorter than 500 nm in samples without Cr^{3+} may be due to Ti^{3+} to which Ti^{4+} could be reduced during the heat treatment. These samples were also used as

blanks for measurements of the absorption spectra of Cr^{3+} in glass-ceramics containing Ti.

Absorption spectra of three glasses and glass-ceramics having different concentrations of TiO_2 are shown in Fig. 2(a-b). Absorption spectra of five samples are given in Fig. 3 (a-e). The samples of mullite glass and glass-ceramics were measured against ordinary undoped glass because it was impossible to prepare identical glass-ceramics without Cr_2O_3.

Optical absorption data are presented in Table 3.

Emission and excitation spectra

Emission and excitation spectra were measured using an Oriel xenon dc 150W lamp; an Oriel 7240 monochromator with a resolution of 6nm/mm blazed at 500nm for excitation of luminescence; a Spex 1704 analyzing monochromator and an RCA 7102 cooled photomultiplier for registration and a PAR 189 selective amplifier and PAR 128 lock-in amplifier for amplification of emission.

All samples were measured in an identical position, namely, when the exciting light fell on the surface of the sample 3mm from the front polished edge. The luminescence was registered from this edge at right angles to the excitation.

All fluorescence spectra were corrected for the spectral response of the instrument by means of a special computer program.

Measurements and calculations of quantum yield were performed by comparison with a standard material of known efficiency [11]. An LLP* glass sample of the same dimensions as the measured glasses, and doped with 0.058 W% of Cr_2O_3 was used as a standard. Quantum efficiency of Cr_2O_3 in this glass was 0.23 [12,13].

In order to eliminate errors connected with the instability of the measuring system the spectra of the standard samples were recorded immediately before and after recording the spectra of the measured samples. Luminescence spectra were taken for different excitation wavelengths.

The spectra of the glasses and glass-ceramics are given in Fig. 4 (a-e)

* lithium lanthanum phosphate

and the quantum efficiency data in Table 3.

The quantum efficiency of Cr^{3+}, defined as the number of photons emitted by Cr^{3+} ions divided by the number of photons absorbed by these ions, is higher than the efficiencies, measured in samples containing high titanium concentrations. The influence of the amount of TiO_2 can be seen in Table 3. In order to circumvent the parasitic absorption of Ti^{3+} it is advisable to reduce the amount of TiO_2 to a minimum, or to exchange it entirely, whenever possible, by a nonabsorbing nucleator.

Fluorescence lifetime measurements

Cr^{3+} fluorescence lifetimes were measured using a tunable dye laser, Molectron DL-200, pumped by a pulsed N_2 laser Molectron UV 14, with a pulse duration of 8ns.

Several dyes were used for different excitation wavelengths: for 525-550nm exc-C485; for 555-565nm-C495; for 595nm-R6G; and for 620-625nm-RB.

The emission passed through a monochromator and was detected with a R928 Hamamatsu photomultiplier. The signal was recovered with a Biomation 8100 digitizer and averaged with Nicolet 178. The signal was observed simultaneously on the Nicolet screen and then recorded on an x-y YEW 3086 recorder.

The first and the second exponential lifetimes τ_{e_1} and τ_{e_2} (defined as the times during which intensity of the luminescence decreases by a factor of e and e^2) were calculated using a computer program (Tables 3).

The integrated lifetimes, defined as:

$$\tau_{int} = \frac{\int_0^\infty tI(t)dt}{\int_0^\infty I(t)dt}$$

where t = time and I = emission intensity, were also calculated. Using these lifetimes, exponential curves were reconstructed. Some of these are represented in Fig. 5 (dotted curves) as compared to measured lifetimes (full curves).

As can be seen from this figure, the difference between the measured and the exponential curves is much higher in glass-ceramics.

II. Discussion

The absorption bands of Cr^{3+} in the crystalline state in the observable $^4A_2 \rightarrow ^4T_2$ transition are shifted to higher energy as compared to the glassy state [3,4]. The oscillator strength in the crystalline phase is generally lower by a factor of two than in the glassy phase. This is not surprising since in the glassy state Cr^{3+} resides in a symmetry lower than in the crystalline, thus allowing more parity-forbidden 3d-3d transitions.

Spinel-type glass ceramics T-51

The emission spectrum of Cr^{3+} in the T-51 spinel type glass-ceramics (Fig. 4(b)), as well as in the other spinel type glass-ceramics [3,4], differs in shape from the emission spectrum of the starting glass (see Fig. 1 of [9]).

The emission spectrum is composed of the $^2E \rightarrow ^4A_2$ emission, which is characteristic for Cr^{3+} in the crystals with a large field strength, and of the wide $^4T_2 \rightarrow ^4A_2$ emission in the glass and low field crystalline sites. The $^2E \rightarrow ^4A_2$ emission reveals a complex structure, which is well resolved at 4 K [8]. In order to understand the origin of various bands we need to know the crystalline structure of spinels and sites into which Cr^{3+} can enter.

The usual "normal spinel" formula is $A^{[4]}B_2^{[6]}X_4$, where A-divalent cation, B-trivalent cation, and X-divalent anion. The symbol [4] designates - tetrahedral coordination and [6] - octahedral coordination. However spinels are known to undergo inversion, the formula of "inverse spinel" being $B^{[4]}[AB]^{[6]}X_4$. The degree of the inversion depends on the conditions of crystallization. Usually it is much larger in synthetic spinels than in natural spinels [14].

In the spinel structure the Cr^{3+} impurities occupy octahedral cation positions([15]). Actually, almost all Cr^{3+} complexes in solutions as well as the solids compounds are known to show the coordination number N=6 with octahedral symmetry [1].

The spinels $MgAl_2O_4$ undergo inversion to some extent when heated between 750°-900° (and higher temperatures) without annealing [14].

The inversion must occur to a considerable degree in our samples as evident from the appearance of additional lines in the spectrum due to $^2E \rightarrow {}^4A_2$ emissions which are the result of changes in the positions of the Cr^{3+} energy levels in the inverted versus normal sites. This behavior in crystals was profoundly studied by Mikenda et al. [14-16].

The intrinsic $^2E \rightarrow {}^4A_2$ luminescence (R-line) has lower intensity, typical for strictly octahedral symmetry, than the Cr^{3+} luminescence in inverted sites [14]. This is not surprising since the parity forbidden transitions become partially allowed when the high symmetry is lowered.

The R-line intensity increases when Cr^{3+} ions are excited at shorter wavelengths. A weak line at ~680nm in the emission spectrum of T-51 glass-ceramics at 555nm excitation is the R line (Fig. 4(b)). This line is missing at 622nm excitation. The next most intensive line at ~690-695nm arises from Cr^{3+} in one of the distorted CrO_6 octahedrons, the most common in our sample. The intensive but almost hidden line at 706nm [the N_2-line [15,17] is due to the exchange-coupled Cr^{3+} ions (emission of Cr^{3+} pairs, like the R line, changes its place only a little in the spectra of different spinels and many other crystals). The origin of this line from the Cr^{3+} pairs is deduced from lifetime measurements and time-resolved spectroscopy at low temperatures [9].

The broad emission at ~700- 1000nm is from Cr^{3+} in the low crystal field (in glass or crystals) - $^4T_2 \rightarrow {}^4A_2$ emission. Its intensity increases relative to the $^2E \rightarrow {}^4A$ group when the excitation is at 622nm. The maximum of the $^4T_2 \rightarrow {}^4A_2$ emission is shifted to a shorter wavelength relative to a simple glass (Fig. 3(a))similarly to absorption; that is, there is a stronger crystal field around Cr^{3+} ions in the

glass-ceramics T-51.

With increasing Cr^{3+} concentration the possibility increases that two Cr^{3+} ions will be in nearby sites interacting antiferromagnetically and creating exchange coupled pairs with characteristic luminescence lines from the ^2E level [8].

The significant exchange pairs Cr^{3+} emission in crystals ordinarily appears when concentration of the dopant is 0.3 mole % [15,18]. In our starting glass the Cr^{3+} concentration is low - only 0.02 mole %. Even at this concentration we observed the N_1 line from pairs in the spinel glass-ceramics. This may be due to the fact that the Cr^{3+} ions are distributed unevenly between crystalline and glassy phases, the crystalline phases being enriched by Cr^{3+} ions. This phenomenon is under further investigation by the ESR method.

The weakness of the R-line in T-51 glass-ceramics may result from energy transfer from single ions to pairs. Energy transfer was also evident from lifetime measurements. The luminescence in T-51 shows high nonexponentiality of the decay curves (Fig.5b and 5c), indicating efficient energy transfer in different time regions between various luminescent centers; in glass, the luminescence is close to exponential [19] (Fig. 5a).

The decay of the R-line emission at 680nm (Table 4) is very steep in the initial time region (τ_{e_1}) because of energy transfer to other Cr^{3+} species. However the duration of luminescence lasts nearly 5ms at room temperature and longer at lower temperatures [9].

The lifetimes of Cr^{3+} ions in distorted sites are usually shorter than for the R-line due to higher transition probability. In our case the lifetime of 696nm luminescence is almost the same as for the R-line, the R-line lifetime being the rate-determining step in this process, governed by energy transfer!

While the high nonexponentiality and duration of the decay curves tell about complicated energy transfer processes between single sites, the same is also true for Cr^{3+} pairs at emission of 706nm. The τ_{e_1} and τ_{e_2} times are much shorter than

for the R-line. Here we can expect thermalization of the ^2E energy level of pairs with the higher crystal field $^4T_2$ level, [1], distribution of energy and shortening of lifetimes.

While the highest Cr^{3+} quantum efficiency in glasses is ~0.23, it is much higher in glass-ceramics [3,4]. This fact, combined with an inexpensive production process, makes glass-ceramics suitable candidates for laser rods and LSC.

The quantum efficiency of Cr^{3+} in the T-51 glass-ceramic is ~1 at 622nm and ~0.6 at 555nm excitation (Table 3), when the effect of Ti^{3+} absorption is excluded. The negative influence of Ti on the apparent quantum efficiency of Cr^{3+} (Table 3) is due to the absorption of Ti^{3+}. We therefore conclude that samples of high efficiency should contain a minimum amount of titania.

Petalite-like type glass-ceramics 3-1

In the glass-ceramic 3-1 Cr^{3+} reveals properties which are characteristic both for high and low field strengths. The main crystalline phases in this type are high (β)-quartz solid solution and petalite-like phase.

The β-quartz is built from SiO_4 tetrahedra, connected in spiral chains [20]. The only way for Cr^{3+} to enter this phase is to occupy interstices in the open quartz structure while Al^{3+} replaces Si^{4+} in the tetrahedra. In such a way Cr^{3+} ions are situated similarly to ordinary glasses; however, they are subjected to a higher surrounding crystal field strength. The absorption and luminescence spectra of Cr^{3+} in β-quartz glass-ceramics are very similar to those in glasses (only shifted to higher energies), and the ^2E luminescence band is slightly more pronounced in the spectrum [3].

The petalite-like phase is a phase with an x-ray pattern similar to that of natural petalite, $LiAlSi_4O_{10}$ [21]. The structure of the natural petalite consists of SiO_4/AlO_4 tetrahedra layers with Li^+ ions in four-fold coordination between them. There are no sites where Cr^{3+} can enter this structure. However, in the petalite-like phase, Mg^{2+} ions replace Li^+, and because Mg^{2+} prefers

octahedral coordination, the petalite-like phase structure may be very distorted from the structure of the natural petalite, allowing entrance of Cr^{3+} ions.

In the system $MgO-Al_2O_3-SiO_2$ in which we are working (Table 2), the pure low quartz does not crystallize, but a whole series of metastable solid solutions which are based on high quartz structures are formed [22]. From these amounts of solutions, after longer periods of heating, more stable crystalline phases are gradually formed. Together with high-quartz solid solution a metastable petalite-like phase, probably with the pyroxene structure, crystallizes [21,23]. In this structure Mg^{2+} ions are in six-fold coordination [24], and may be replaced by Cr^{3+}. In this manner, Cr^{3+} ions may occupy different crystalline sites in different crystalline phases of 3-1 glass-ceramics, and reveal characteristic spectroscopic properties with diffused emission bands.

The origins of the various emission bands can be obtained by analogy with the works of W. Mikenda et al. [14-17].

The emission band at ~675-680nm (Fig. 4(c)). can be attributed to the undistorted R-line with the highest energy and the band at 705nm to the emission of the pairs of Cr^{3+} ions from the same sites. The large concentration of such pairs is deduced from the intensity of this emission. The most intensive line at ~690nm is from the Cr^{3+} ions in other crystalline sites, while emission at ~715nm originates from the corresponding Cr^{3+} pairs with a much lower concentration. The broad $^4T_2 - {}^4A_2$ emission is weak at 550nm excitation and increases with longer wavelength excitations. It is also shifted to the higher energies on comparison with starting glass (Fig. 4(c)).

The lifetimes of Cr^{3+} in the 3-1 glass-ceramics are shorter than in T-51 (Table 4) and lasts only 2 msec at room temperature. The R-line lifetime is shortened because of possible energy transfer to Cr^{3+} pairs. The lifetimes of the 690nm and 705nm emissions are similar, while that of the 715nm emission is much shorter. It reveals decreasing lifetimes of the pairs but very likely

may be caused by thermalization with the closely situated $^4T_2$ level. The lifetime of $^4T_2$ itself is of the ordinary value- about 10μs.

The quantum efficiency of Cr^{3+} in petalite-like glass ceramics is high: up to 0.8-0.9, while Cr^{3+} efficiency in the starting glass is only 0.2 (Table 3). The Ti absorption decreases the efficiency of Cr^{3+} luminescence to 0.5-0.7 but it is still large. It is also possible to decrease the amount of TiO_2 in the system, which upon crystallization gives petalite-quartz type glass-ceramics. We can consider this type of glass-ceramics suitable for LSC and laser purposes because of its high quantum efficiency and intensive broad luminescence.

Zirconia type glass-ceramics Z-1 and T-Z4

In the glass-ceramics Z-1 and T-Z4, ZrO_2 crystallizes tetragonally (T)[25]. The coordination number of Zr^{4+} is 8. There are no ion sites with coordination number 6. Also we cannot see any interstitial site with such a coordination. The conclusion is that in this glass-ceramics there is no space for Cr^{3+}, requiring coordination number 6. During crystallization, Cr^{3+} ions must remain in the residual glassy phase. This means that Cr^{3+} ions are exposed to low field strength in zirconia glass-ceramics as confirmed by broad low intensive luminescence from the $^4T_2$ level identical to the $^4T_2 \rightarrow {}^4A_2$ Cr^{3+} luminescence in glasses (Fig. 4d). Also the luminescence lifetimes are the same (Table 4) as in glasses.

The considerable change of colour followed by decrease of optical denisty and oscillator strength in this glass-ceramics, as compared to glass, is not understood. It could be perhaps due to partial oxidation of Cr^{3+} to Cr^{6+}. All the above discussion concerns T-Z4 glass-ceramics. The large concentration of Cr_2O_3 in this sample gives the glass and glass-ceramics a dark colour, decreases the luminescence efficiency and shortens the lifetimes.

Mullite type glass-ceramics, M

The conditions of preparation and the composition range for mullite glass-ceramics in which Cr^{3+} has an intensive emission were studied in the excellent

works of Beall et. al. [26-28]. In this paper we present for the first time detailed spectroscopic measurements and analysis of Cr^{3+} doped mullite glass-ceramics.

The crystalline phase of the glass-ceramics M has the stoichiometric formula $2Al_2O_3 \cdot SiO_2$. Aluminium ions occupy both tetrahedral and octahedral sites [29] each type forming chains. Usually mullite is not a pure compound and dissolves variable amounts of SiO_2 and other substances.

Chromium ions enter octahedral sites replacing Al^{3+}. Emission of Cr^{3+} (Fig. 4a) is very broad and intensive with one distinct peak at 697nm. Obviously this emission originates from the Cr^{3+} ions situated in different sites of high field strength ($^2E \rightarrow {}^4A_2$) as well as low strength ($^4T_2 \rightarrow {}^4A_2$). By comparison with spinels it was concluded that 683nm emission originates from undistorted Cr^{3+} sites (the R-line). 697 emission is from Cr^{3+} in the most frequently met distorted sites, having lifetimes longer than lifetimes of the R-line (Table 4). The other lines, due to pairs, are obscured by the broad emission from the $^4T_2$ level, which also shifts to shorter wavelengths comparative to glass.

The lifetime of Cr^{3+} in the starting glass is usual for the $^4T_2$ emission - 6μs (Table 4), and very long in the glass-ceramics with duration of luminescence up to 5ms.

The nonexponentiality of all decay curves indicates slow energy transfer between various centers. τ_{e_1} and τ_{e_2} of the R line is shorter than for the 697 line because of energy transfer to the exchange coupled pairs in this higher Cr^{3+} doped sample (Table 2). The lifetimes of the emission at 725nm (where there is no distinct line) are shorter - it may be ^2E emission of Cr^{3+} in high distorted sites, which are known for shorter lifetimes, and also emission from $^4T_2$ in a sufficiently large field, which is in thermal equilibrium with the ^2E level. The lifetimes are shortened for the 750nm emission ($^4T_2$) and also for the larger wavelengths' excitations (565nm, 625nm).

The quantum efficiency of Cr^{3+} in the starting glass is 0.14 (Table 3). It is the usual value for 0.1 mole% Cr^{3+} in glass. The quantum efficiency of Cr^{3+} ions in mullite glass-ceramics is as high as ~1.0. This fact together with width of emission and absence of TiO_2 makes mullite glass-ceramics one of the most suitable for LSC* and lasers.

III. Present and Future Work

The main conclusion which we can infer is that glass-ceramics represent high potential media for the introduction of Cr^{3+} ions, which is very interesting from both the theoretical and practical points of view. Glass-ceramics of definite spinel types, petalite and mullite types, already deserve more detailed investigation for their possible utilization. The others meanwhile require more precise laboratory work. We think that the present and future work must consist of the following points:

1. ESR investigation of the samples. This will help to determine the Cr^{3+} distribution between residual glass and crystalline phases and also reveal different Cr^{3+} sites in the different glass-ceramics types.
2. Exclusion of TiO_2 in the glass-ceramics by other nucleator agents, such as ZrO_2 and better, by P_2O_5. Investigation of systems which may give transparent glass-ceramics only by phase separation processes without introduction of nucleators (mullite types, for example).
3. Achieval of greater amounts of crystalline phases by minor changes in compositions and heat treatment. It will help to determine Cr^{3+} sites in these phases more precisely and also optimize luminescence intensities.
4. Change of Cr^{3+} concentrations. It is necessary to investigate possible limits of Cr^{3+} concentration, in which Cr^{3+} absorption increases without causing concentration quenching. It will reveal the optimum concentrations accompanied by the most intensive emission. On the other hand increasing concentrations will help to study different crystalline sites occupied by Cr^{3+} ions.

* luminescent solar concentrator

Acknowledgement

The authors are grateful to Prof. C.K. Jørgensen for fruitful discussions, to Dr. Robert Katz for his support and encouragement and to Dr. M. Eyal for the computer program.

The authors are also very grateful to Mr. and Mrs. Willy Berler for their kind support of the work in this laboratory.

1. R.Reisfeld,Proc.Advanced Summer School on the Electronic Structure of New Materials,Loviisa,August 1984.Report no.40,Swedish Academy of Engineering Sciences in Finland,Helsinki,1985,pp.7-34.
2. R.Reisfeld,Mater.Sci.and Eng. 71(1985)375.
3. R.Reisfeld,A.Kisilev,E.Greenberg,A.Buch and M.Ish-Shalom, Chem.Phys.Lett. 104(1984)153.
4. A.Kisilev,R.Reisfeld,E.Greenberg,A.Buch and M.Ish-Shalom, Chem.Phys.Lett. 105(1984)405.
5. A.Buch,M.Ish-Shalom,R.Reisfeld,A.Kisilev and E.Greenberg, Mater.Sci.and Eng. 71(1985)383.
6. R.Reisfeld,A.Kisilev,C.K.Jørgensen,A.Buch and M.Ish-Shalom,Abstracts 167.Meeting Electrochem.Soc.,Luminescent and Display Materials Group, Toronto,Canada,May 1985.
7. R.Reisfeld,A.Kisilev,A.Buch and M.Ish-Shalom,Chem.Phys.Lett. 129(1986)446.
8. A.Kisilev,R.Reisfeld,A.Buch and M.Ish-Shalom,Chem.Phys.Lett.129(1986)45(
9. M.Bouderbala,G.Boulon,R.Reisfeld,A.Buch,M.Ish-Shalom and A.M.Lejus, Chem.Phys.Lett. 121(1985)535.
10. A.P.Syritskii et al.,Izv.Akad.Nauk SSSR,Neorg.Mater.19[12](1983)2031.
11. R.Reisfeld,J.Res.Nat.Bur.Stand. A 76(1972)613.
12. A.Kisilev and R.Reisfeld,Solar Energy 33(1984)163.
13. R.Reisfeld and A.Kisilev,Chem.Phys.Lett. 115(1985)457.
14. J.Derkosch,W.Mikenda and A.Preisinger,Spectrochim.Acta 32 A(1976)1759.
15. W.Mikenda and A.Preisinger,J.Lumin. 26(1981)53 and 67.
16. W.Mikenda,J.Lumin. 26(1981)85.
17. J.Derkosch and W.Mikenda,J.Lumin. 28(1983)431.
18. G.F.Imbusch,in:Energy Transfer Processes in Condensed Matter,ed. B.DiBartolo,Plenum Press,New York,1984,p.47.
19. R.Reisfeld,in:Spectroscopy of Solid State Laser-type Materials, ed. B.DiBartolo (Plenum,to be published).
20. W.D.Kingery,H.K.Bowen and D.R.Uhlmann,"Introduction to Ceramics", 2.ed. (Wiley,New York,1976).
21. W.Schreyer and J.F.Schairer,Am.Mineralogist 47(1962)90.
22. W.Schreyer and J.F.Schairer,Z.Kristallogr. 116(1961)60.
23. B.G.Varschal,L.G.Baiburt,A.M.Gelberger,N.N.Malachovskaya and A.P. Naumkin,J.Neorganischeskie Materialy 7(1971)4.
24. A.S.Povarennykh,Crystal Chemical Classification of Minerals(Plenum, New York,1972)p.409
25. D.K.Smith and H.W.Newkirk,Acta Cryst. 18(1965)983.
26. G.H.Beall,J.F.MacDowell and M.P.Taylor,US Patent 4396720(1983).
27. G.H.Beall,J.Non-Cryst.Solids 73(1985)413.
28. G.H.Beall,N.F.Borelli and D.L.Morse,US Patent 4526873(1985).
29. R.Sadanaga,M.Tokonami and Y.Takeuchi,Acta Cryst. 15(1962)65.

TABLE 1

Ligand Field Parameter Δ (in the unit 1000cm^{-1}) for CrO_6 in Glass Ceramics (g.c.), Solids and Complexes in Solution.

Spinel-type g.c.	original glass	15.5
-do. -	glassy micro-phase	15.95
-do. -	micro-crystallites	17.25
β-quartz g.c.	glassy micro-phase	16.0
-do. -	micro-crystallites	16.8
petalite-like g.c.	original glass	15.6
-do. -	glassy micro-phase	16.0
-do. -	micro-crystallites	17.5
various silicate glasses		15.2-15.5
lithium lanthanum phosphate glass		15.45
Alexandrite $Al_{2-x}Cr_xBeO_4$		17.35
Spinel $MgAl_{2-x}Cr_xO_4$		18.2
Spinel-type $MgAlCrO_4$		17.65
Ruby $Al_{2-x}Cr_xO_3$ ($x<0.04$)		18.0
greyish pink $Al_{1.6}Cr_{0.4}O_3$		17.55
$Cr(C_2O_4)_3^{-3}$ (oxalate complex)		17.5

TABLE 2 Compositions, Heat Treatments and Crystalline Phases in the Cr^{3+} Doped Glass Ceramics.

Glass	Amounts (mol%) of oxides in glass											Nucleation		Crystallization		Crystalline phases in glass-ceramics	
	SiO_2	Al_2O_3	B_2O_3	MgO	CaO	ZnO	K_2O	TiO_2	ZrO_2	As_2O_3	Cr_2O_3	Temperature(°C)	Soaking time(h)	Temperature(°C)	Soaking time(h)	Major	Minor
T-51	48.7	19.4	-	19.5	-	-	-	8.6	3.8	-	0.026	750	10	950	2	Spinel	β-quartz SS* ZrO_2(T)**
3-1	58.7	16.7	-	17.8	-	-	-	3.7	3.0	-	0.026	780	10	920	2	β-quartz SS	petalite-like phase ZrO_2(T)
Z-1	47.2	10.1	-	-	-	35.2	-	-	7.5	-	0.029	730	10			ZrO_2(T)	-
T-Z4	49.0	19.6	-	-	19.6	-	-	6.0	5.8	-	0.028	750	10	900	2	ZrO_2(T)	
M	63.0	13.5	19.8	-	-	-	3.6	-	-	0.012	0.045	790	10	900	2	Mullite	-

* SS - solid solution

** T - tetragonally

Table 2

TABLE 3

Spectral characteristics and quantum efficiencies η of chromium(III) in glasses (g.) and glass-ceramics (g.c.). The molar extinction coefficient ε is given for absorption maxima, and the oscillator strength f of the $^4A_2$-$^4T_2$ (derived from the absorption band area) is given in the unit 10^{-4}. η_{Cr} refers to the quantum efficiency evaluated for the absorption in the Cr(III) only, and η_{Cr+Ti} the smaller value obtained, taking into account the absorption by simultaneously present titanium.

Sample		Phases after heat treatment	Absorption			Luminescence		
			λ(nm)	ε	f	λ_{exc} (nm)	η_{Cr}	η_{Cr+Ti}
T-51	(g.)	-	660	37.3	2.48	-	-	-
	(g.c.)	Spinel ZrO_2(T)	600	15.0	2.6	622	~1.0	0.32
						555	0.60	0.24
J-1	(g.)	-	680	11.0	1.46	625	~0.2	~0.18
			490	23.9				
	(g.c.)	β-quartz; petalite-like phase; ZrO_2(T)	680	7.8	-	625	0.90	0.70
			490	31.2		550	0.33	0.51
Z-1	(g.)	-	660	24.8	2.12	-	-	-
			395	7.5				
	(g.c.)	ZrO_2(T)	665	10.9	0.78	625	0.20	-
			395	18.1				
T-24	(g.c.)	ZrO_2(T)	665	28.6	3.28	633	0.21	0.18
			445	~215				
M	(g.)	-	620	30.1	3.48	625	0.14	-
			410	28.2				
	(g.c.)	mullite; residual glass	620	15.6	3.3	625	~1.0	-
						592	0.56	-

TABLE 4

Life-time Data on Chromium(III) in Glasses and Glass-Ceramics. Wave-lengths of emission λ_{em} and λ_{exc} are given in nm. The life-times τ_1 and τ_2 (in microseconds) refer to the time where the intensity is 1/e and $1/e^2$ of the intensity immediately following the exciting flash. The duration (in milliseconds) refer to the (much longer) time, when the luminescence still can be detected (corresponding to energy storage in the long-lived ^2E state)

Sample	Main phases	λ_{em}	λ_{exc}	τ_1	τ_2	duration
LLP	glass	830	625	22	28	0.1
T-51	spinel	677-680	555	200	488	5
		696	555	220	437	5
		706	555	117	330	5
		712	555	88	151	2.5
3-1	β-quartz; minor amounts of petalite-like phase	675-680	595	48	95	1
		685-690	550	58	160	2
			595	90	174	2.5
		705	550	74	159	2
		715	595	26	48	1
		765	595	12	17	0.1
			625	4	6	0.05
Z-1, glass		835	625	16	19	0.1
Z-1,	ZrO_2(T)	697	625	12	17	0.1
		750	625	9	14	0.1
		820	625	7	12	0.1
M, glass		835	625	6	7	0.1
M,	mullite	683	525	298	470	5
			565	124	204	2.5
			625	88	160	2.5
		697	525	366	650	5
			565	160	248	2.5
			625	134	200	2.5
		725	525	160	254	5
		750	565	42	66	1
			625	85	130	2.5

FIGURE CAPTIONS

Fig.1. X-ray diffraction of the translucid glass-ceramics samples. 1: T-51; 2: Z-1; 3: T-Z4; 4: 3-1; 5: M.
On the curves: z: ZrO_2(T); s: spinel; q: β-quartz; p: petalite-like phase; m: mullite.

Fig.2. Absorption spectra of undoped glasses and glass-ceramics with different amounts of TiO_2.The mole percent is 1.5 on part a, and 6 and 10.8 on part b.

Fig.3.Absorption spectra of chromium(III) in different glasses and glass-ceramics containing 0.05 mole percent Cr_2O_3.The parts are a: T-51; b: 3-1; c: Z-1; d: T-Z4; e: M.

Fig.4. Emission spectra of chromium(III) in different glasses and glass-ceramics containing 0.05 mole percent Cr_2O_3.The life-times indicated are the second-fold exponential life-times τ_2.The parts are a: LLP glass; b: T-51; c: 3-1; d: Z-1 and T-Z4; e: M.

Fig.5. Decay curves of samples containing 0.05 mole percent Cr_2O_3. The full curves are measured;the curves with small black circles correspond to purely exponential curves with the same integrated life-times.The parts are
a: LLP glass excited at 625 nm,emission measured at 830 nm.
b: T-51 glass-ceramics excited at 555 nm,emission measured at 696 nm.
c: Also T-51 glass-ceramics excited at 555 nm,but the emission measured at 712 nm.

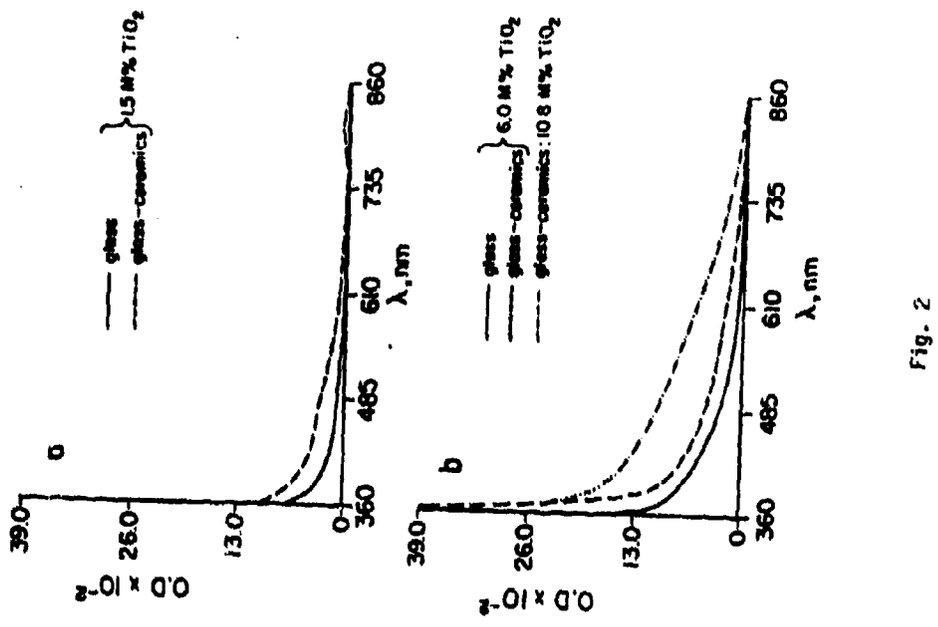
a
glass
glass-ceramics } 1.5 M% TiO2
O.D x 10-2
39.0
26.0
13.0
0
360
485
610
735
860
λ, nm
b
glass
glass-ceramics } 6.0 M% TiO2
glass-ceramics: 10.8 M% TiO2
O.D x 10-2
39.0
26.0
13.0
0
360
485
610
735
860
λ, nm

Fig. 2

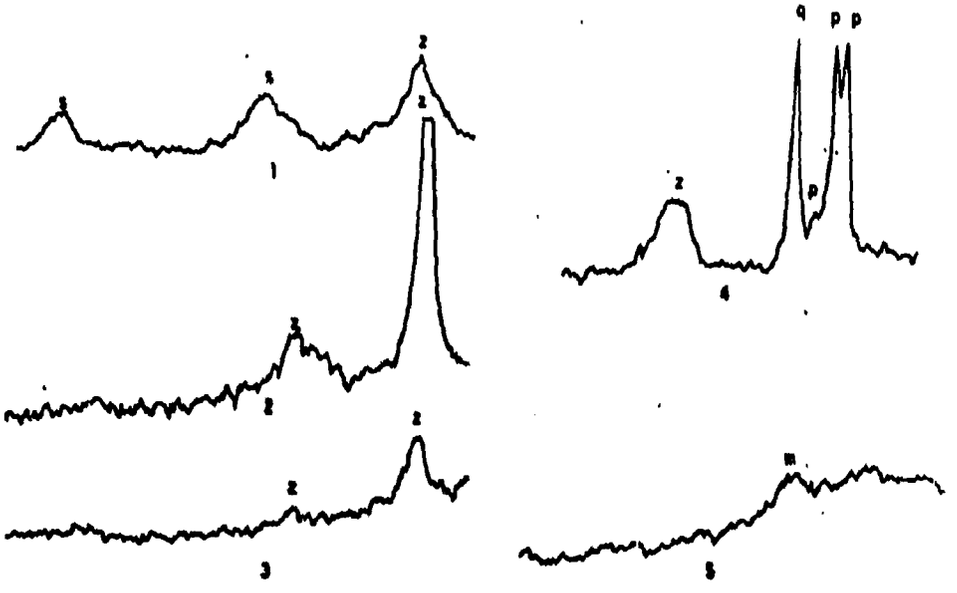
1
2
3
4
5
p

Fig. 1

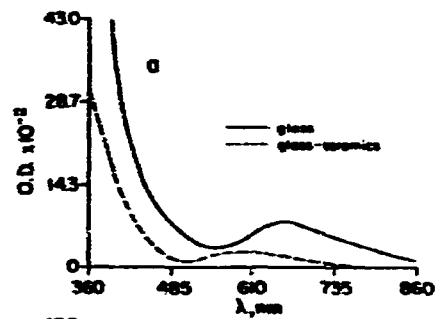
a
O.D. x10⁻²
430
287
143
0
360
485
610
735
860
λ,nm
glass
glass-ceramics

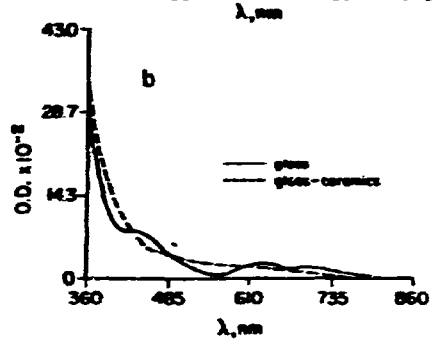
b
O.D. x10⁻²
430
287
143
0
360
485
610
735
860
λ,nm
glass
glass-ceramics

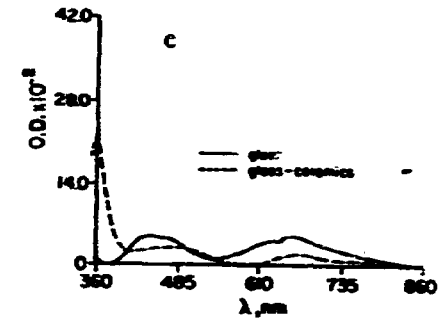
c
O.D. x10⁻²
420
280
140
0
360
485
610
735
860
λ,nm
glass
glass-ceramics

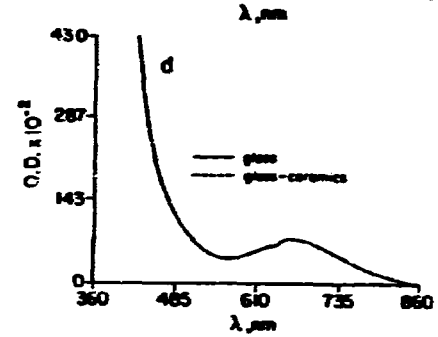
d
O.D. x10⁻²
430
287
143
0
360
485
610
735
860
λ,nm
glass
glass-ceramics

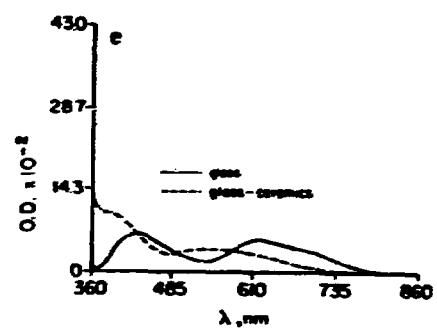
e
O.D. x10⁻²
430
287
143
0
360
485
610
735
860
λ,nm
glass
glass-ceramics

Fig. 3

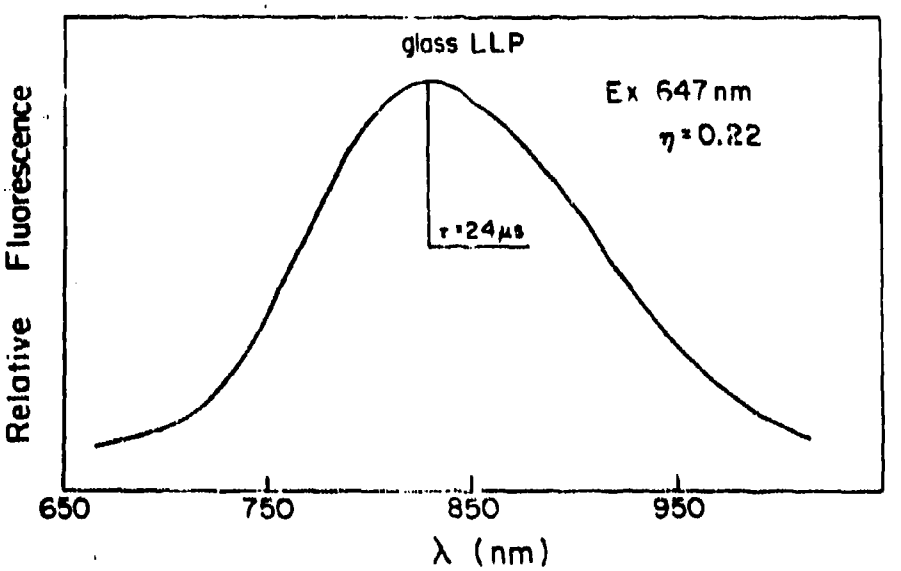
glass LLP
Ex 647 nm
η = 0.22
τ = 24 μs
Relative Fluorescence
650
750
850
950
λ (nm)

Fig. 4a

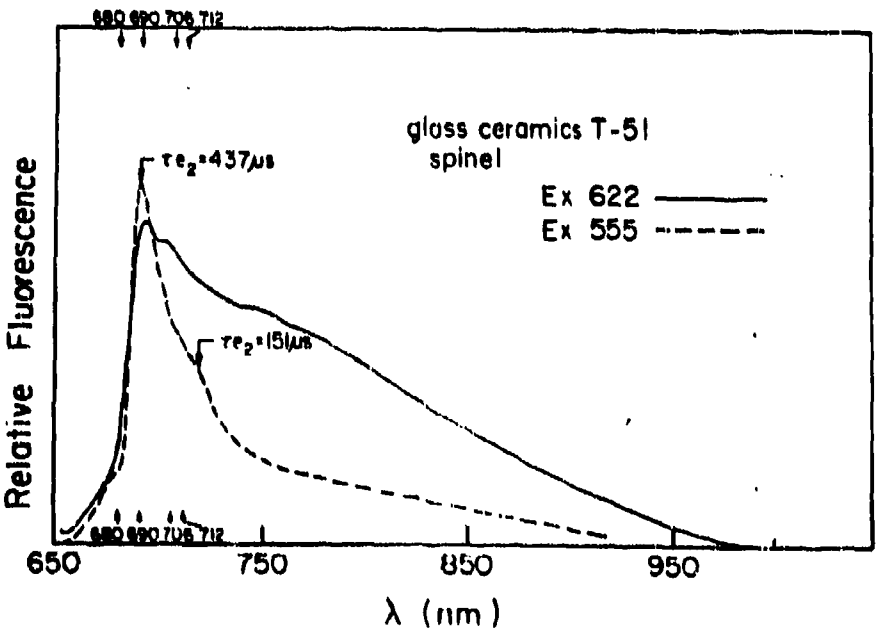
680 690 706 712
glass ceramics T-51
spinel
Ex 622
Ex 555
τe2 = 437 μs
τe2 = 151 μs
Relative Fluorescence
650
750
850
950
λ (nm)

Fig. 4b

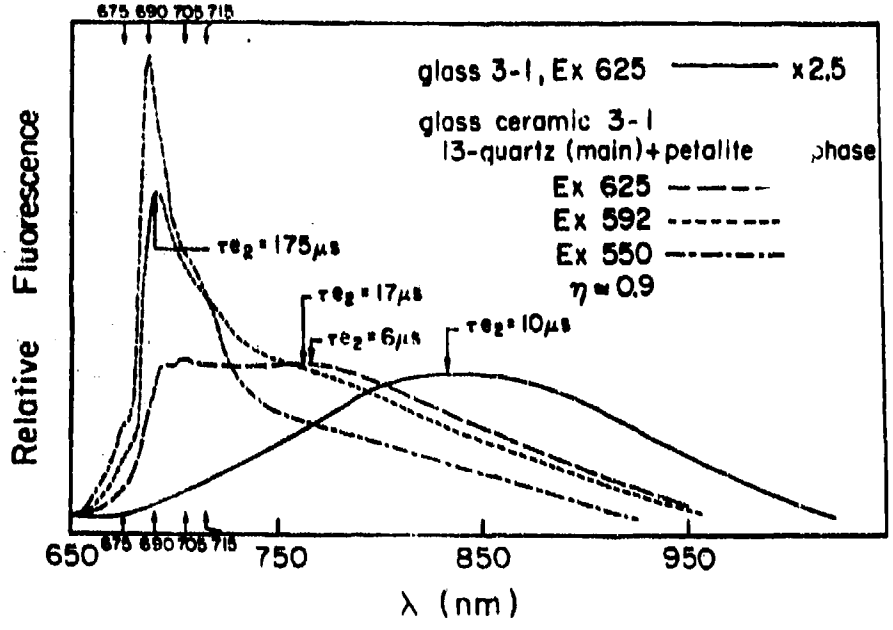
675 690 705 715
glass 3-1, Ex 625 ——— x2.5
glass ceramic 3-1
13-quartz (main)+petalite phase
Ex 625 — — —
Ex 592 - - - - - -
Ex 550 — · — · —
η ≈ 0.9
τe2 = 175μs
τe2 = 17μs
τe2 = 6μs
τe2 = 10μs
Relative Fluorescence
650
675 690 705 715
750
850
950
λ (nm)

Fig. 4c

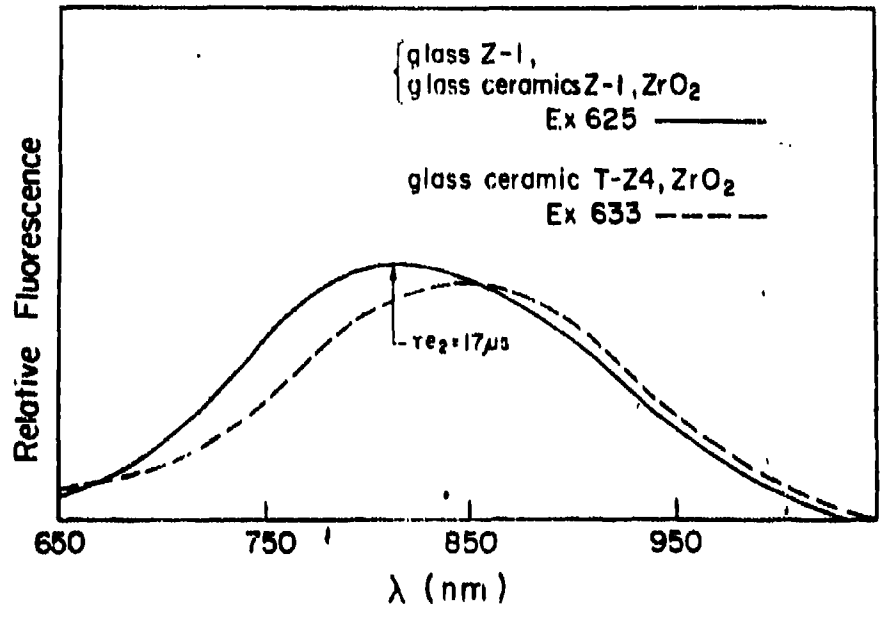
glass Z-1,
glass ceramics Z-1, ZrO2
Ex 625 ———
glass ceramic T-Z4, ZrO2
Ex 633 — — —
τe2 = 17μs
Relative Fluorescence
650
750
850
950
λ (nm)

Fig. 4d

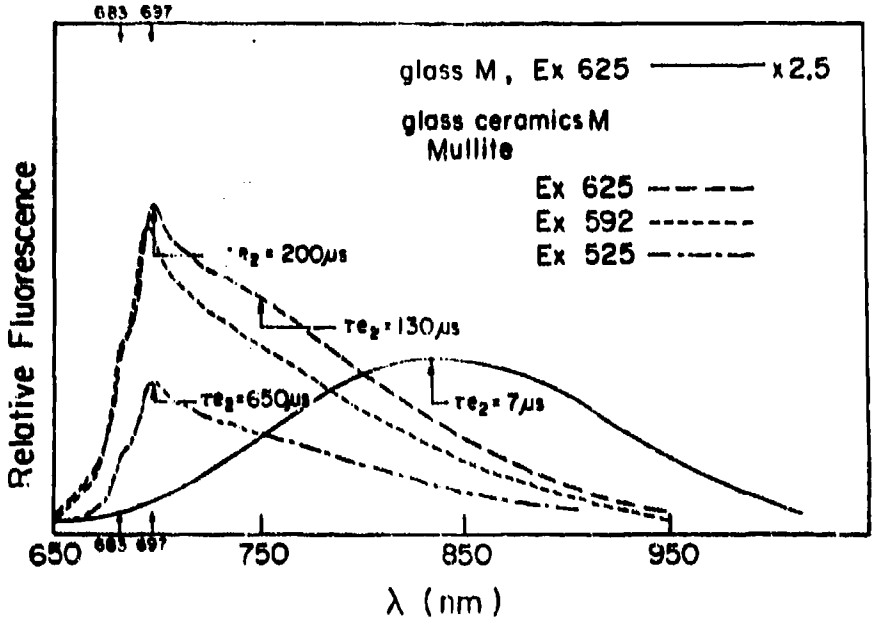
683 697
glass M, Ex 625 ——— x2.5
glass ceramics M
Mullite
Ex 625 – – –
Ex 592 -------
Ex 525 —·—·—
τ_{e_2} = 200μs
τ_{e_2} = 130μs
τ_{e_2} = 650μs
τ_{e_2} = 7μs
Relative Fluorescence
650
683 697
750
850
950
λ (nm)

Fig. 4e

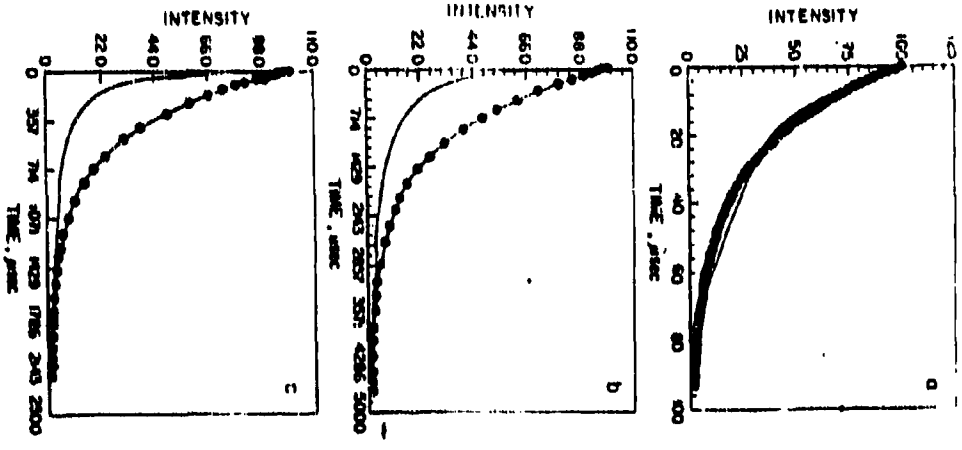
INTENSITY
INTENSITY
INTENSITY

Fig. 5

Volume 129, number 5 CHEMICAL PHYSICS LETTERS 12 September 1986

SPECTROSCOPY AND EPR OF CHROMIUM(III) IN MULLITE TRANSPARENT GLASS-CERAMICS *

R. REISFELD[1], A. KISILEV
Department of Inorganic and Analytical Chemistry, The Hebrew University of Jerusalem, Jerusalem 91904, Israel

A. BUCH and M. ISH-SHALOM
Israel Ceramic and Silicate Institute, Technion City, Haifa 32000, Israel

Received 6 June 1986; in final form 8 July 1986

Mullite glass-ceramics were prepared with varying concentrations of Cr(III). The X-ray absorption, emission and EPR spectra reveal that the most defined crystals are formed at the lowest concentration of Cr(III). The concentration quenching of the luminescence is small and the quantum efficiencies high as compared with glasses.

1. Introduction

It has been shown in a number of recent papers that quantum efficiencies of Cr(III) at room temperature in transparent glass-ceramics are much higher than in corresponding glasses [1–7]. This fact is attributed to small probabilities of non-radiative relaxation in more organized glass-ceramics. Similarly the concentration quenching of fluorescence of the $^4T_2 - {}^4A_2$ emission is high in glasses [8–10] and much lower in glass-ceramics. It is the purpose of the present work to study the influence of Cr(III)-doped mullite glass-ceramics [3–5] and to verify the conclusions by parallel study by X-ray diffraction and EPR measurements. The knowledge accumulated on spectroscopy in ruby [11] is helpful in the interpretation of our results.

2. Experimental

The glass-ceramics were prepared by the usual method of thermally treating a precursor glass. A glass of basic composition [4] was used: $45SiO_2$: $20B_2O_3$:$25Al_2O_3$:$9.95K_2O$:$0.05As_2O_3$ (all quantities in weight per cent). The various amounts of Cr_2O_3 were added to this basic mixture as given in table 1.

In order to prepare the glasses 100 g portions of mixtures were melted in alumina crucibles in an electrical furnace heated to 1600°C, then poured into a steel mold and put in a furnace preheated to 650°C for annealing. The furnace was immediately turned off and glasses were cooled at the cooling rate of the furnace.

In the preparation of the mullite glass-ceramics three Cr(III) concentrations were used. The concentrations are listed in table 1; they are designated by symbols 3B, 25B and 26B. The heat treatment was performed in two steps as follows: First heating at 700–750°C for 2 h and then at 800°C for 4 h. The heated glasses were cooled at the cooling rate of the furnace. Plates of 10×10×3 mm dimensions were cut and polished. X-ray diffraction spectra were measured on a Philips diffractometer using Cu Kα radiation with a Ni filter. Absorption, emission and excitation spectra and quantum efficiencies were measured as in refs. [1,2]. EPR spectra were taken at room temperature on a Varian E-12 EPR spectrophotometer at 9.17 GHz with 10 mW power. The magnetic field was varied from 500 to 4500 G.

* Supported by US Army Contract No. DAJA 45-85-C-0031.
[1] Enrique Berman Professor of Solar Energy.

Table 1
Spectroscopic properties of Cr(III) in mullite glass-ceramics containing different amounts of Cr_2O_3

Assignment	Concentration of Cr_2O_3			Absorption		Emission	
	W%	M%		wavelength λ(nm)	OD (for 1 mm)	wavelength of excitation λ(nm)	quantum efficiency
3B	0.05	0.024	glass	630	0.028	625	0.19
			glass	600	0.014	625	0.58
			ceram.	390	0.014	560	1.00
25B	0.1	0.047	glass	630	0.058	625	0.07
			glass	600	0.030	625	0.71
			ceram.	390	0.026	560	0.91
26B	0.3	0.095	glass	630	0.120	625	very low
			glass	600	0.066	625	0.65
			ceram.	390	0.067	560	0.84

3. Results and discussion

The X-ray diffraction spectra are in fig. 1. Characteristic peaks due to mullite crystals can be seen distinctly. At higher concentrations of Cr_2O_3 the X-ray patterns are more diffuse than at low concentration. This behaviour is opposite to that of Cr(III)-doped spinel glass-ceramics [6,12]. In the latter case Cr_2O_3 stabilizes spinel crystals and may be used as a nucleator when it is added in sufficiently large amounts. We succeeded also in preparation of mullite glass-ceramics of the same composition undoped by Cr(III). The crystallites were bigger; after the same heat treatment the glass-ceramics were a little opalescent. The conclusion is: in the case of mullite glass-ceramics the crystallization continues immediately after liquid–liquid phase separation without the nucleation step [13].

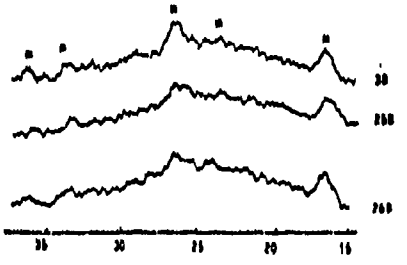

Fig. 1. X-ray diffraction spectra of mullite containing glass-ceramics with various amounts of Cr_2O_3. m = mullite.

On the other hand, Cr_2O_3 is known as one of the most active surface agents for lowering the surface tension [14,15]. Cr_2O_3 additions to original undoped mullite glass-ceramics may decrease surface tension on the border of two liquid phases, decrease internal energy, change mutual liquid phase distribution and finally cause a decrease of the crystalline size.

The position and intensities of absorption peaks of Cr(III) depend on the degree of crystallization. In glasses the absorption of the $^4A_2 \rightarrow {}^4T_2$ transition peaks at 630 nm and the optical density of a 1 mm thick plate is about twice that of the glass-ceramics of identical thickness and concentration (table 1).

The resulting absorbance in glass-ceramics is the sequence of many factors, such as Cr_2O_3 distribution between glasses and crystalline phases, shift of absorbance bands to shorter wavelength in glass-ceramics as a result of stronger ligand field, and decrease of oscillator strength for higher symmetry. In the glass-ceramics 3B the absorption spectrum is moved to shorter wavelengths than in the sample 26B which resembles the glass.

Emission spectra are shown in fig. 2 for two excitation wavelengths: 625 and 560 nm. The dominant emission at 560 nm excitation in the glass-ceramics 3B is the emission at 698 nm from the ^2E energy level. It occurs at longer wavelengths than is known for Cr(III)-doped crystals: ruby [11,16], alexandrite [17] and different spinels [3,18], and may be a conse-

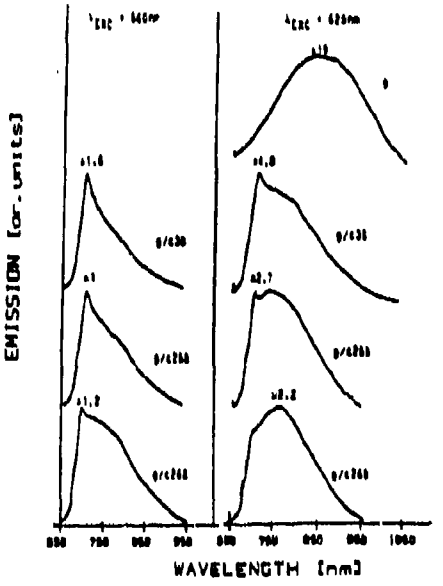

Fig. 2. Emission spectra of mullite glass-ceramics, doped to different concentration by Cr(III). g = glass, g/c = glass-ceramics.

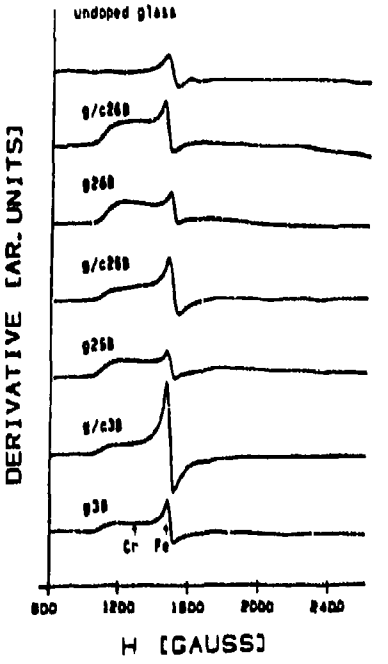

Fig. 3. EPR derivative spectra (measured at $\nu \approx 9.17$ GHz) of unheat-treated glasses and mullite glass-ceramics, doped to different concentrations by Cr(III). g = glass, g/c = glass-ceramics.

quence of lower symmetry. The part of $^4T_2$ emission is also essential. In the 25B and 26B samples the $^4T_2$ emission is more and more pronounced. This behaviour is more notable at 625 nm excitation, when the $^4T_2$ level is directly excited. For this excitation $^4T_2$ emission is dominant in glass-ceramics 26B. In all these cases emission intensities are much larger than for ordinary Cr(III)-doped glasses.

EPR behaviour (fig. 3) is less obvious than emission. Mullite glass-ceramics lack high-symmetry sites as spinels and gahnite [1,3] and subsequently lack the characteristic signal at nearly 1580 G. The signal at 1460 G originates from Fe^{3+} [12]; it appears also in undoped glasses and glass-ceramics (fig. 3). The concentration increase is clear in glasses as well as in glass-ceramics. In the crystallized samples the left sides of the wide signal are slightly decreased and the right-peak signal is much enlarged. It is known from ref. [12] that the Fe^{3+} signal does not change after crystallization, so such a behaviour must reflect a change of derivative in consequence of Cr(III) entering into the crystalline phases. This change becomes less and less pronounced at larger Cr(III) concentrations.

The most important question is concentration quenching and quantum efficiencies at larger concentrations of Cr_2O_3. It is shown in table 1. The quantum efficiencies of Cr_2O_3 in glasses are given for comparison. The strongest concentration quenching is in glasses. Quantum efficiencies of Cr(III) in mullite glass-ceramics are very high (see also ref. [3]). It is 1 at 560 nm excitation in sample 3B, a little smaller for sample 25B. On the other hand, efficiency at 625 nm excitation is even higher in the second glass-ceramics sample. However, they both decrease in the next sample, containing 0.2 W% ($\approx$ 0.1 M%) Cr_2O_3.

Although there is only a small decrease in quantum efficiencies, the decrease starts already at a low concentration. It is obvious that the cause of it is in the decreasing concentration of Cr(III) in the crystalline phase together with a general decrease of amounts of this phase. Therefore it is not like the common behaviour for other types of glass-ceramics. In such types of glass-ceramics as gahnite, spinel, petalite in which Cr_2O_3 stabilizes the crystalline phase, the concentration threshold may be very high. It is also worth noting that the observed concentration quenching does not reject the potential utilization of mullite glass-ceramics: together with this small decrease of quantum efficiencies the Cr(III) absorbance increases significantly, so, the overall emission also increases.

References

[1] R. Reisfeld, A. Kisilev, E. Greenberg, A. Buch and M. Ish-Shalom, Chem. Phys. Letters 104 (1984) 153.

[2] A. Kisilev, R. Reisfeld, E. Greenberg, A. Buch and M. Ish-Shalom, Chem. Phys. Letters 105 (1984) 405.

[3] A. Kisilev and R. Reisfeld, J. Non-Cryst. Solids, to be published.

[4] G.H. Beall, J.F. MacDowell and M.P. Taylor, U.S. Patent 4396720 (1983), Corning Glass Works, USA.

[5] G.H. Beall, N.F. Borrelli and D.L. Morse, U.S. Patent 4526873 (1985), Corning Glass Works, USA.

[6] F. Durville, B. Champagnon, E. Duval and G. Boulon, J. Phys. Chem. Solids 46 (1985) 701.

[7] M. Bouderbala, G. Boulon, R. Reisfeld, A. Buch, M. Ish-Shalom and A.M. Lejus, Chem. Phys. Letters 121 (1985) 535.

[8] A. Kisilev and R. Reisfeld, Solar Energy 33 (1984) 163.

[9] L.J. Andrews, A. Lempicki and B.C. McCollum, J. Chem. Phys. 74 (1981) 5526.

[10] R.H. Clarke, L.J. Andrews and H.A. Frank, Chem. Phys. Letters 85 (1982) 161.

[11] G.F. Imbusch, Phys. Rev. 153 (1967) 326.

[12] R.S. Abdarakhmanov, E.M. Konoval and I.V. Shishkin, Fiz. Khim. Stekla 9 (1983) 403.

[13] J.F. MacDowell and G.H. Beall, J. Am. Ceram. Soc. 52 (1969) 17.

[14] I.I. Kitaigorodsky, Technology of glass (1961) p. 38.

[15] A.M. Gelberger, N.M. Vaisfeld and B.I. Varshal, Neorg. Mat. 5 (1969) 340.

[16] G.F. Imbusch, in: Energy transfer processes in condensed matter, ed. B. Di Bartolo (Plenum Press, New York, 1984) p. 47.

[17] J.C. Walling, H.P. Jenssen, R.C. Morris, E.W. O'Dell and O.G. Peterson, Opt. Letters 4 (1979) 182.

[18] W. Mikenda and A. Preisinger, J. Luminescence 26 (1981) 53.